THE ROLE OF N-LINKED GYCOSYLATION

DURING *DROSOPHILA* DEVELOPMENT

by

Allison F. McCague

A thesis submitted to the Faculty of the University of Delaware in partial fulfillment of the requirements for the degree of Honors Bachelor of Science in Biological Sciences with Distinction

Spring 2013

THE ROLE OF N-LINKED GYCOSYLATION

DURING *DROSOPHILA* DEVELOPMENT

by

Allison F. McCague

Approved: _____

Dr. Erica M. Selva, PhD
Professor in charge of thesis on behalf of the Advisory Committee

Approved: _____

Dr. David W. Smith, PhD
Committee member from the Department of Department Name

Approved: _____

Dr. Rolf D. Joerger, PhD
Committee member from the Board of Senior Thesis Readers

Approved: _____

Michael Arnold, Ph.D.
Director, University Honors Program

ACKNOWLEDGMENTS

I firmly believe that the most important factor to an undergraduate's success in research is the right mentor. I am so lucky to have found the greatest mentor I could have ever asked for in Dr. Erica Selva. As both my research mentor and my academic advisor, she has given me her undying support from day one of this process. This final product would not have been possible without her guidance. Not only did I have an amazing mentor, I also had a fantastic lab group helping me through this process. No research project is ever the work of one person, so I would like to thank my lab mates (past and present) for all of their help and support. Net, Erica, Alicia, Nick, Joe, Sencer, and Babak: you guys made my years in the Selva lab so enjoyable and I know working in the lab in the future won't be the same without you. Having a second family in my lab group has meant so much to me.

I would also like to thank my second and third readers, Dr. David Smith and Dr. Rolf Joerger. Your advice throughout this process has been truly invaluable and I am very grateful for the amount of time you both have invested in my academic achievement by taking on the endeavor of being on my committee. I am also so incredibly fortunate to have a remarkable support network of family and friends in my corner, celebrating my successes and encouraging me through challenges and obstacles. For dealing with me throughout this process and helping me maintain my sanity, my family, my roommates, and my friends have my undying gratitude. Finally, I would like to thank University of Delaware's Undergraduate Research Program, Howard Hughes Medical Institute, and the National Science Foundation for providing

me with the funding to pursue this research. Completing a research project and writing a senior thesis has been by far the most rewarding endeavor of my undergraduate career. This process and everyone that has helped me along the way have not only made me a better academic, but also a better person. Armed with the knowledge and confidence this undertaking has given me, I look forward to starting a new chapter in my career as an aspiring scientist as a PhD student at Johns Hopkins.

TABLE OF CONTENTS

LIST OF TABLES

LIST OF FIGURES

ABSTRACT

N-linked glycosylation is a key post-translational modification for many secretory pathway targeted proteins. Endoplasmic reticulum glycosyltranferases construct a 14-sugar precursor on a dolichol carrier, which is transferred *en mass* to nascent peptides on asparagine consensus sites. *Drosophila alg9* and *alg10* N-glycosylation mutants were used to examine the role of this modification during development of the fly. The *alg10* gene encodes the enzyme catalyzing terminal glucose addition to the sugar-precursor prior to transfer, while *alg9* encodes an enzyme acting five steps earlier. In embryos, the loss of *alg9* and *alg10* causes severe and pleotrophic defects. Central nervous system (CNS) neurons were specified in both *alg9* and *alg10* embryos. Loss of *alg10* disrupted axon pathfinding, while *alg9* embryos lacked mature neurons. *Drosophila* eye development in the absence of *alg9* and *alg10* yielded small rough adult eyes, but the *alg9* phenotype was more severe. Rescue of the *alg10* rough eye phenotype by eye-specific expression of an *alg10* transgene confirmed that the eye phenotype was caused by the loss of *alg10*. Examination of molecular markers in *alg9* and *alg10* late 3rd instar eye imaginal discs suggested adult small rough adult eyes might be due to neuronal apoptosis. These eye discs also showed defects in axon pathfinding, as shown by the loss of Bolwig's nerve and disrupted axon tracks. All of these results are consistent with the hypothesis that loss of *alg10* may disrupt the maturation of a subset of N-glycoproteins, while *alg9* is essential for most or all N-glycoproteins, since it acts earlier and has far more severe developmental defects.

Chapter 1

INTRODUCTION

1.1 The N-Linked Glycosylation Pathway

Asparagine- or N-linked glycosylation is a key post-translational modification for many eukaryotic proteins, targeted to the secretory pathway, which play important roles in cell recognition and signaling during development. The oligosaccharide substrate for N-glycosylation is assembled at the membrane of the endoplasmic reticulum (Figure 1). A 14-sugar lipid linked oligosaccharide (LLO) is constructed on a dolichol carrier by a series of glycosyltransferases. Subsequently, an amide linkage is formed between *N*-acetyleglucosamine (GlcNAc) and consensus asparagine sites on the target protein. Upon being transferred to nascent proteins on consensus asparagine sites, the glycan contains two GlcNAc, nine mannose, and three glucose units. The protein-bound glycan is then trimmed of its terminal glucose by a glucosidase (GLS1). The glycan is then trimmed of the other two glucose units, yielding $mannose_8$-$GlcNAc_2$-protein, before being modified further in the Golgi apparatus, where many enzymes compete for the same substrate, thus creating the potential for many N-glycan structures. The final structure is determined by the specific target protein, cell-specific expression, and numerous other factors (Freeze, 2006).

Previous studies using yeast have identified the genes encoding the specific glycoslytransferases needed to assemble the final oligosaccharide. Characterization of these yeast glycosyltransferase mutants revealed deficiencies in N-linked glycosylation, particularly in the assembly of the lipid-linked oligosaccharide. These

mutants are called *alg* mutants (Haeuptle & Hennet, 2009). When such *alg* mutations were combined with a conditional mutation in oligosaccharyltransferase activity - the enzyme that transfers the fully glycosylated substrate to an asparagine in nascent protein - the result was a lethal phenotype. We are applying this knowledge of the N-linked glycosylation pathway and *alg* mutants to a higher eukaryote, *Drosophila melanogaster* and examining the effect of *alg10* and *alg9* on development. Previous studies on other loci in the pathway, such as *alg5*, showed that reduced glycosylation in *alg5* mutants triggers endoplasmic reticulum stress and the unfolded protein response (UPR) that occurs as a result of an accumulation of unfolded proteins in the endoplasmic reticulum (Shaik et al., 2011). This accumulation results in specific patterning defects during embryonic development.

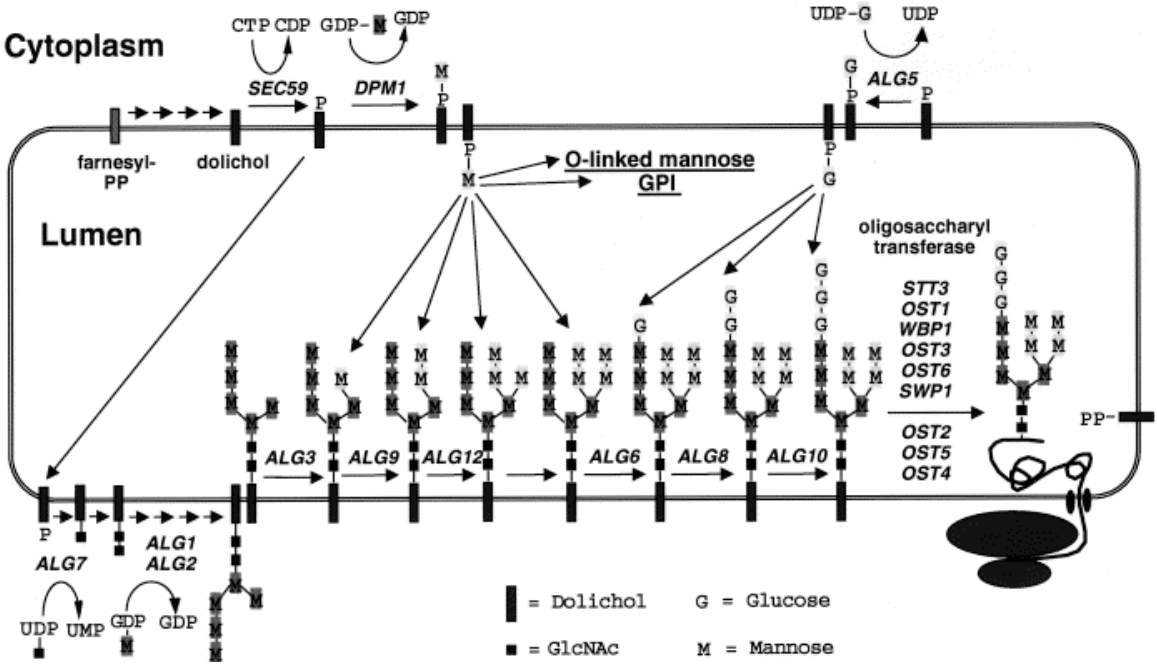

Figure 1. **The N-linked glycosylation pathway.** Alg10 catalyzes the addition of the terminal glucose reside to the dolichol-linked ogliosaccharide in the ER just prior to transfer to nascent polypeptides during N-glycosylation. (Figure adapted from Burda and Aebi, 1999).

1.2 *Asparagine-Linked Glycosylation 9 and 10*

Asparagine-Linked Glycoslyation 10 (*alg10*) is a gene encoding an α-1,2 glycosyltransferase, which catalyzes the addition of the terminal glucose reside to the dolichol-linked oligosaccharide in the endoplasmic reticulum just prior to transfer to nascent polypeptides during N-glycosylation, yielding the fully assembled core oligosaccharide acting just downstream of Alg5 (Figure 1). In *Drosophila* it is located on the left arm of chromosome 3 and is 1,649 base pairs long. The final protein product is 473 amino acids long; it is a multipass transmembrane protein between the ER lumen and the cytoplasm.

Asparagine-Linked Glycosylation 9 (*alg9*) encodes an α-1,2-mannosyltransferase, which adds a mannose residue to the α-1,3-linked mannose and acts five steps earlier in the N-linked pathway than Alg10. It is a hydrophobic protein containing 7 transmembrane domains and has two potential glycosylation sites on the ER lumen side. It uses dolichol-P-Man as the donor substrate (Haeuptle & Hennet, 2009). In *Drosophila* it is located on the right arm of chromosome 3, is 2,529 base pairs long, and encodes a final protein product 611 amino acids in length.

I hypothesized that defects in *alg9* will be more severe than defects in *alg10* due to the existence of two isoforms in *Drosophila* of oligosaccharyl transferase (OST), the enzyme responsible for the transfer of the complete oligosaccharide to nascent peptides. OST-A will only take fully glycosylated substrates, while OST-B can transfer underglycosylated substrates (Figure 2) (Shrimal 2013). In cells expressing isoform B, Alg10 activity would not be predicted to be required for transfer, while neither isoform will transfer an oligosaccharide produced in the absence of Alg9 activity, producing a more severe phenotype.

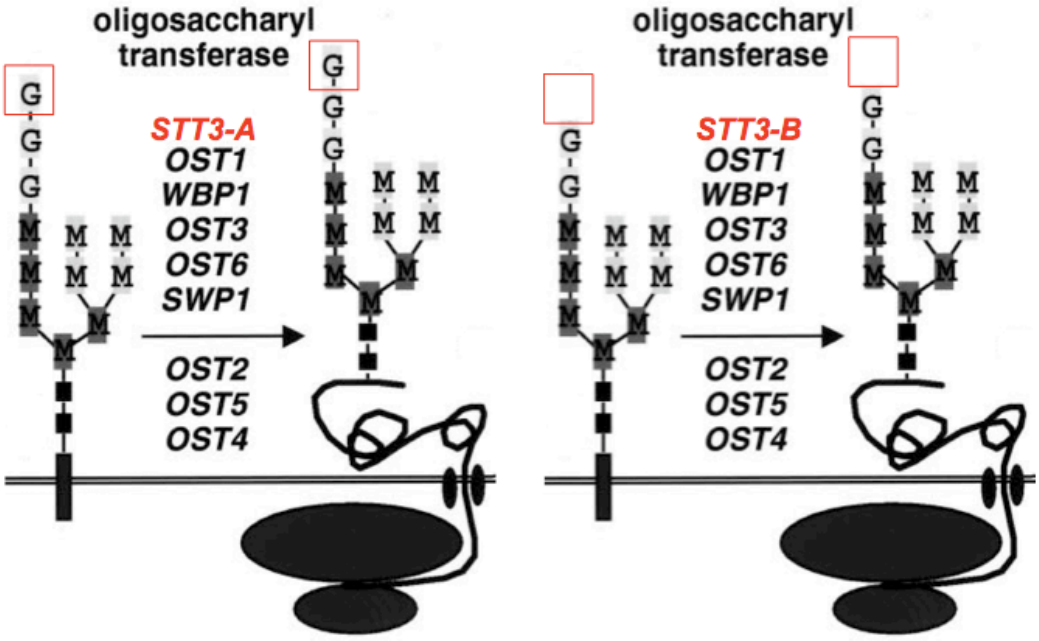

Figure 2. **The two isoforms of oligosaccharyl transferase.** The A isoform can only transfer fully glycosylated substrates, whereas the B isoform can transfer underglycosylated substrates. (Figure adapted from Burda and Aebi, 1999).

1.3 Congenital Disorders of Glycosylation: A Novel Model

As the N-linked glycosylation pathway is conserved from *Drosophila* to humans and defects in N-glycosylation in humans lead to diseases known as congenital disorders of glycosylation (CDG), this work also has translational implications for human disease. In the past 20 years, approximately 1,000 CDG patients have been identified, presenting with more than 200 mutations in 15 different genes, resulting in over 30 distinct genetic diseases (Haeuptle & Hennet, 2009). However, identifying CDG patients is often difficult because of their rarity and the fact that symptoms vary widely in type and severity. For this reason, the impact of CDGs is likely more far-reaching than is currently appreciated.

The mortality rate for disorders in N-linked glycosylation is approximately 20% in the first 5 years of life, after which point the mortality rate sharply decreases. All known CDGs show autosomal recessive inheritance. CDGs are divided into two groups: I and II. Type I CDGs involve defects in glycan synthesis, whereas type II CDGs involve defects in glycan processing (Freeze, 2006). While a CDG associated with *alg10* has yet to be identified, CDGs have been found for *alg6* and *alg8*, the genes which encode the other two ER membrane glycosyltransferases in the pathway. While the ALG6-CDG (CDG-Ic) is relatively common (the second most frequent form of CDG) and presents with moderate symptoms (psychomotor retardation, developmental delay, seizures, hypotonia, coagulopathy, feeding problems, and visual impairment), the ALG8-CDG (CDG-Ih) leads to a very severe form of the disease that is deadly within the first 5 months of life for a majority of patients (Haeuptle & Hennet, 2009).

A CDG associated with *alg9* has also been identified: CDG-Il. There are only three known cases of this CDG and there is not enough data to draw any clinical conclusions about this CDG; however, symptoms associated with CDG-Il patients have included developmental delay, psychomotor retardation, hypotonia, seizures, hepatomegaly, microcephaly, and pericardial effusion (Haeuptle & Hennet, 2009). A type II CDG (CDG-IIb) has also been identified for *GLS1*, which encodes the glucosidase responsible for trimming the terminal glucose of the protein-bound glycan in the ER. The symptoms of this CDG include dysmorphism, hypotonia, seizures, hepatomegaly, and hepatic fibrosis. This CDG is lethal within the first 2.5 months of life (Freeze, 2006). A list of all known Type I CDGs and their associated defective genes and proteins is found in Table 1. By using *Drosophila* to model this poorly

understood group of genetic disorders, we can glean more insight into their mechanisms and effects, which can lead to better therapies and higher life expectancy.

Table 1. **Identified Type I congenital disorders of glycosylation.** Genes directly or indirectly connected with our work are highlighted in yellow. (Table adapted from Haeuptle and Hennet, 2009.)

Disorder	Defective Gene	Defective Protein	Mutations	Patients
CDG-Ia	*PMM2*	Phosphomannomutase 2	103	>800
CDG-Ib	*MPI*	Mannose phosphate isomerase	18	>25
CDG-Ij	*DPAGT1*	GlcNAc-1-P transferase	3	3
CDG-Ik	*ALG1*	Mannosyltransferase 1	4	7
CDG-Ii	*ALG2*	Mannosyltransferase 2	2	1
CDG-Id	*ALG3*	Mannosyltransferase 6	9	11
CDG-Il	*ALG9*	Mannosyltransferase 7-9	2	3
CDG-Ig	*ALG12*	Mannosyltransferase 8	11	8
CDG-Ic	*ALG6*	Glycosyltransferase 1	20	>36
CDG-Ih	*ALG8*	Glycosyltransferase 2	12	9
CDG-Im	*DOLK*	Dolichol kinase	2	4
CDG-Ie	*DMP1*	Dolichol-P mannosyltransferase 1	6	8
CDG-Io	*DMP3*	Dolichol-P mannosyltransferase 3	1	1
CDG-If	*MPDU1*	Man-P-dolichol utilization defect 1	5	5
CDG-In	*RFT1*	RFT1 homolog (*S. cerevisiae*)	5	6

1.4 *Drosophila* as a Model Organism

Ever since the work of Thomas Hunt Morgan at the beginning of the 20th century paved the way for the discovery of sex-linked inheritance and the ability to cause mutation via ionizing radiation, *Drosophila melanogaster* has been a favorite model organism for geneticists. Many of the same reasons flies were studied in the

early 20th century still apply today, along with new discoveries that make the fruit fly the perfect organism to study developmental genetics.

Perhaps the most obvious advantage of flies is that they are less costly and time consuming to upkeep than more complicated models, such as mice. Stocks can be maintained relatively easily and cheaply and flies have a very short generation time (Figure 3), producing many offspring in a short period of time. Additionally, not only are flies simpler to upkeep than mice, they are simpler genetically. *Drosophila* only has four chromosomes, only three of which make a significant contribution to the genome. Furthermore, its entire genome has been sequenced and it has been found that approximately 75% of human disease-related loci have a *Drosophila* ortholog (Stephenson & Metcalfe, 2013). Therefore, research done on *Drosophila* is translational and can apply to problems in human health. Tools such as FlyBase provide the *Drosophila* community with a database of genetic and molecular data, available for anyone who wants to study *Drosophila*.

Because of its genetic simplicity, *Drosophila* has given geneticists many genetic tools that are very useful for scientific research, including balancer chromosomes, the UAS/GAL4 system, and the FLP/FRT system, which are discussed in greater detail in subsequent sections.

1.4.1 The *Drosophila* Life Cycle

Drosophila has four morphologically distinct developmental stages: embryo, larva, pupa, and adult (Figure 3). The larval stage has three instar phases. Embryogenesis, the first instar larval stage, and the second instar larval stage each last one day. The third instar larval stage lasts two days. After the pupa forms, metamorphosis lasts four days and then a sexually mature fly emerges. In total, the

time from fertilization to hatching of the adult fly is about 10 days at room temperature (Tennessen & Thummel, 2011).

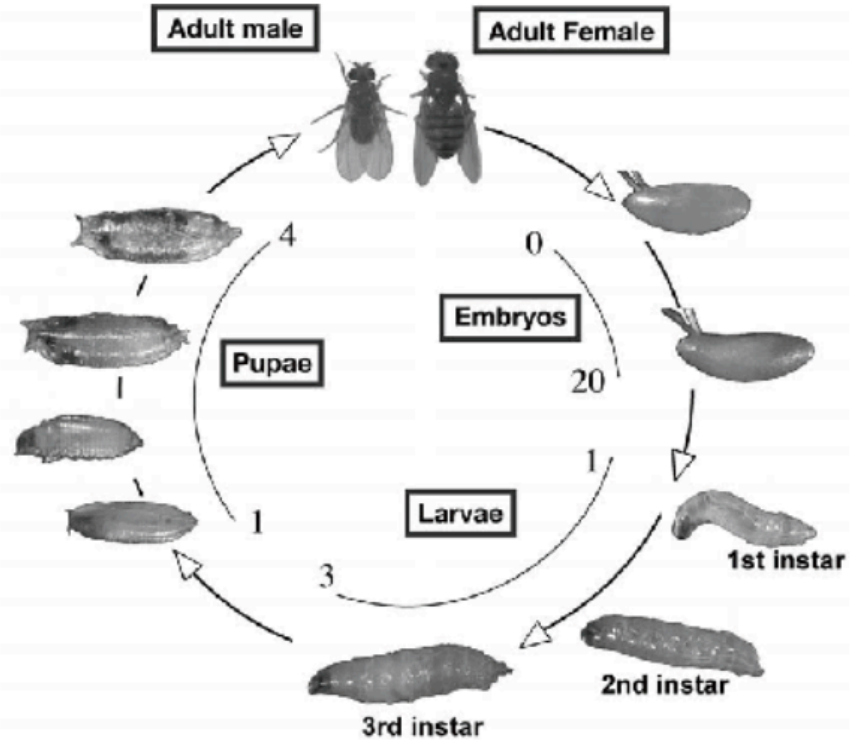

Figure 3. **The *Drosophila* life cycle.** The time from fertilization to the hatching of the adult fly is approximately 10 days. (Figure adapted from (Fernández-Moreno et al., 2007).

1.4.2 Balancer Chromosomes

One of the many genetic tools discovered and used in *Drosophila* is the use of balancer chromosomes. A balancer chromosome is a chromosome that has three principal properties: the presence of an inversion loop that suppresses the production of viable recombination products, the existence of a recessive lethal mutation that eliminates homozygous balancer flies from the population, and a dominant phenotypic

marker that distinguishes flies that receive the balancer from other flies in the population (Hentges & Justice, 2004).

Balancer chromosomes are vital to genetic studies in *Drosophila* for several reasons. Firstly, their use in mutagenesis screens is invaluable. Mutagenesis driven by chemical mutagens, such as ethyl methanesulfonate (EMS) can produce mutations anywhere in the genome, yielding many phenotypes. Because balancer chromosomes repress recombination, lethal mutations can be maintained as a balanced stock if they are located on the homolog of the balanced chromosome. This enables mutagenesis screens to be performed, whereby the location of the mutation can be identified (Hentges & Justice, 2004).

This property of repression of recombination products (hence the term "balancer"), combined with the presence of the recessive lethal mutation that eliminates homozygous balancer flies from the population enables fly geneticists to maintain mutations that would ordinarily be homozygous lethal as balanced stocks (Figure 4) (Hentges & Justice, 2004). The use of balancer chromosomes is therefore very important to stock maintenance.

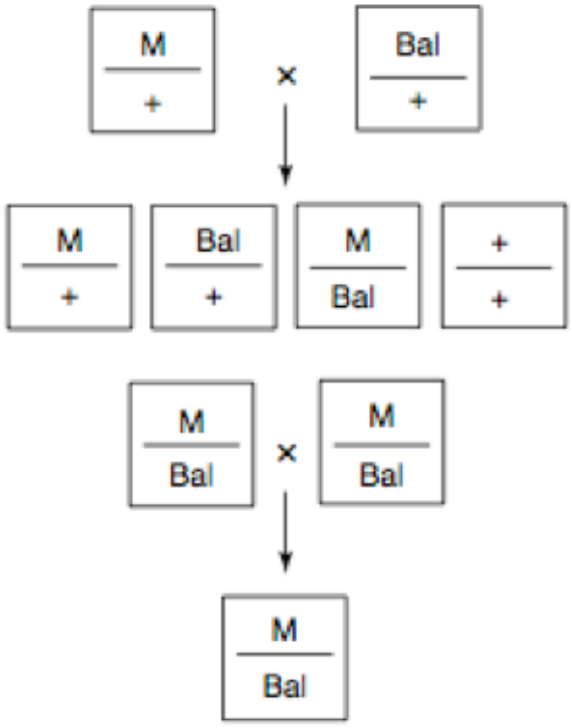

Figure 4. **The use of balancer chromosomes in stock maintenance.** Crossing a stock containing a homozygous lethal mutation (M) with a stock containing a balancer (Bal) on the same chromosome, which also contains a recessive lethal mutation, only yields three types of progeny (balancer alone, mutant and balancer together, and mutation alone). By selecting for flies which contain the mutation and the balancer, a mutation can be maintained as a balanced stock. (Figure adapted from Hentges & Justice, 2004).

Not only can the use of balancer chromosomes maintain stocks, they can also be used to identify mutants. Due to the presence of a dominant phenotypic marker, flies that receive the balancer can be distinguished from flies that do not. This enables inheritance of the chromosome to be easily tracked through subsequent crosses (Hentges & Justice, 2004). These dominant phenotypic markers can be used through

many developmental stages, as balancer chromosomes exist that contain larval markers, such as *Tubby (Tb)*, which results in shorter and fatter larvae than those of the wild type, or that contain adult markers, such as *Stubble (Sb)*, which produces flies that have shorter hairs on the thorax than those of the wild type, or *Curley (Cy)*, which results in curly wings.

1.4.3 The FLP/FRT System

Another genetic tool commonly used by *Drosophila* developmental geneticists is use of the FLP/FRT system to create germline clones and mosaic organisms. Wherever FLP (a site-specific recombinase) is expressed, mitotic recombination is induced at FLP recombination target (FRT) sites on the chromosome, creating daughter cells that are either mutant or wild type (Figure 5). FLP constructs are often expressed under the control of a heat shock promoter in order to control the induction of mitotic recombination events, which allows for high levels of FLP to be expressed during the developmental stage of interest. When marked with cell-autonomous markers, clones can be easily identified and their developing tissues analyzed (Theodosiou & Xu, 1998).

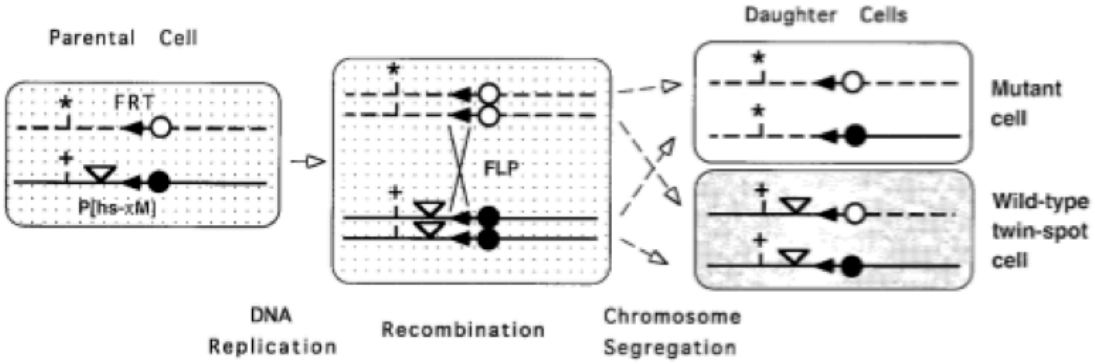

Figure 5. **Generating mutant clones using the FLP/FRT system.** In a heterozygous parent cell (far left), FLP induces mitotic recombination between FRT sites (solid black arrowheads) on homologous chromosome arms. Segregation of recombinant chromosomes during mitosis produces two types of daughter cells: mutant cells containing two copies of the mutant allele (*) and wild-type twin-spot cells containing two copies of the wild-type allele (+). These two types of cells divide further to produce clones. The cell marker (white arrowhead) co-segregates only with the wild-type allele, thus enabling its identification in subsequent cell divisions. The mutant, by contrast, lacks this marker and can be distinguished by the marker's absence. (Figure adapted from Theodosiou & Xu, 1998)

There are many advantages to the FLP/FRT system. The use of this system allows multifunctional genes to be analyzed for their roles throughout development, instead of in adult clones alone. The FLP/FRT system also allows for the comparison of mutant tissue and wild type tissues side-by-side. Additionally, FRT sites proximal to the centromere have been introduced onto each major chromosome arm, allowing this technique to be used for almost any gene of interest. Furthermore, this technique allows for an improvement in traditional genetics screens, which required three generations of crosses to establish individual lines for identifying potential mutants.

The FLP/FRT system allows for mutations to be identified in one generation (Theodosiou & Xu, 1998). Additionally, the requirement later in development for many genes that are lethal to the embryo when homozygous can be analyzed, which is essential for this study.

1.4.3.1 Generating Germline Clones Using the ovoD Method

The maternal contribution (often referred to as "maternal load") of RNA and protein is essential for embryonic development. However, these contributions often make it difficult to determine the earliest stage of development that a particular gene product is required. However, the discovery of *ovoD* opened the door to eliminating the effects of the maternal load. *OvoD* is a dominant female sterile mutation that is germline-specific; the presence of a single copy of *ovoD* creates atrophic ovaries that do not produce eggs, thus blocking oogenesis at an early stage. The *ovoD* chromosome made it possible to create germline clones via homologous recombination, thus circumventing the contribution of the maternal load. Combining the use of this chromosome with the FLP/FRT system described in section 2.2.3 increases the efficiency of germline clone production via heat shock-driven expression of the site-specific recombinase FLP to promote recombination at FRT and to produce germline stem cells that have the mutation in question on both homologous chromosomes and lack *ovoD*. Of the three recombinant products of FLP-catalyzed site-specific exchange post-DNA replication, only the one containing two copies of the mutation produces eggs (Figure 6) (Selva & Stronach, 2007).

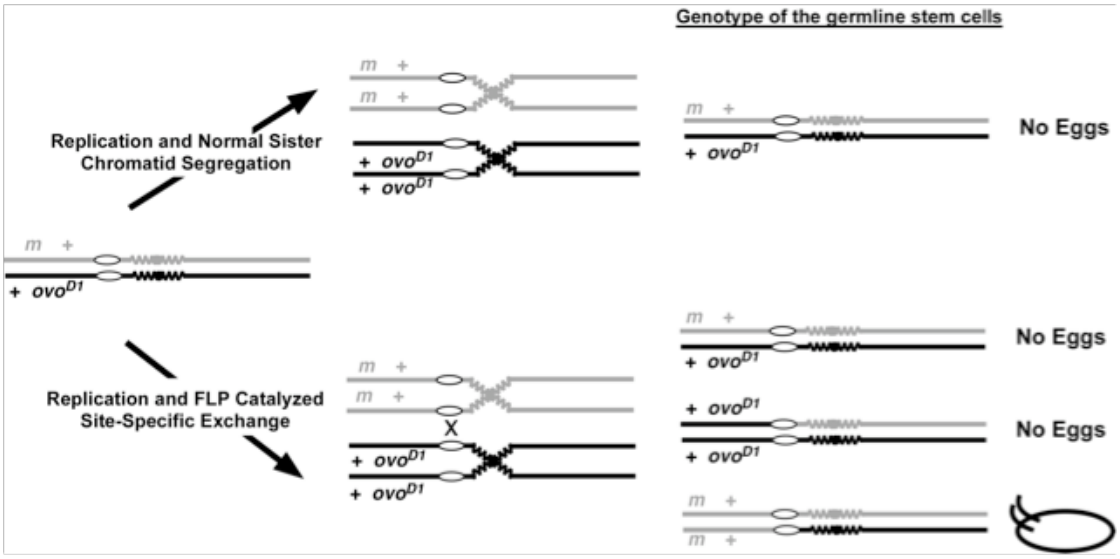

Figure 6. **Generating germline clones using the *ovoD* method.** Combining the *ovoD* mutation with the FLP/FRT system allows for the efficient production of germline clone embryos, whereby only the recombinant germline stem cells containing two copies of the mutation produces eggs. (Figure adapted from Selva & Stronach, 2007).

ovoD mutations have been introduced on every major chromosome arm, thus allowing this method to be used for almost any gene of interest (Theodosiou & Xu, 1998). Because no equivalent of this technique yet exists for the male germline, males heterozygous for the mutation in question must be used, which yields a mixed population of both fully mutant and paternally rescued embryos, receiving the wild type allele from the heterozygous father. However, it is often advantageous to be able to compare fully mutant phenotypes with paternally rescued phenotypes side-by-side. Fully mutant embryos are identified in immunofluorescent staining by the absence of the marker on the balancer chromosome (described in section 1.4.2).

1.4.4 The UAS/GAL4 System

First discovered in *Saccharomyces cerevisiae*, *GAL4* encodes a transcription factor of 881 amino acids that regulates gene expression by binding to upstream activator sequences (UAS). In *Drosophila*, *GAL4* expression is also capable of stimulating transcription of a reporter gene under UAS control (Duffy, 2002). The development of this system has allowed fly geneticists to control target gene expression in a temporal and spatial fashion. In the UAS/GAL4 system, expression of the gene of interest is controlled by the presence of the UAS, which only activates genes in the presence of *GAL4*. To utilize the system, lines with the gene of interest downstream of the UAS are mated to lines expressing *GAL4* in a certain pattern, which is called the driver (Figure 7). The resulting progeny express the gene of interest in the same pattern that *GAL4* expression is controlled by endogenous enhancers (Duffy, 2002). The *GAL4* gene has been inserted at random positions in the *Drosophila* genome through P-element mediated transposition to generate "enhancer trap" driver lines that express *GAL4* under the control of nearby genomic enhancers, and there is now a large collection of driver lines that express *GAL4* in a large variety of cell-types and tissue-specific patterns (St. Johnston, 2002).

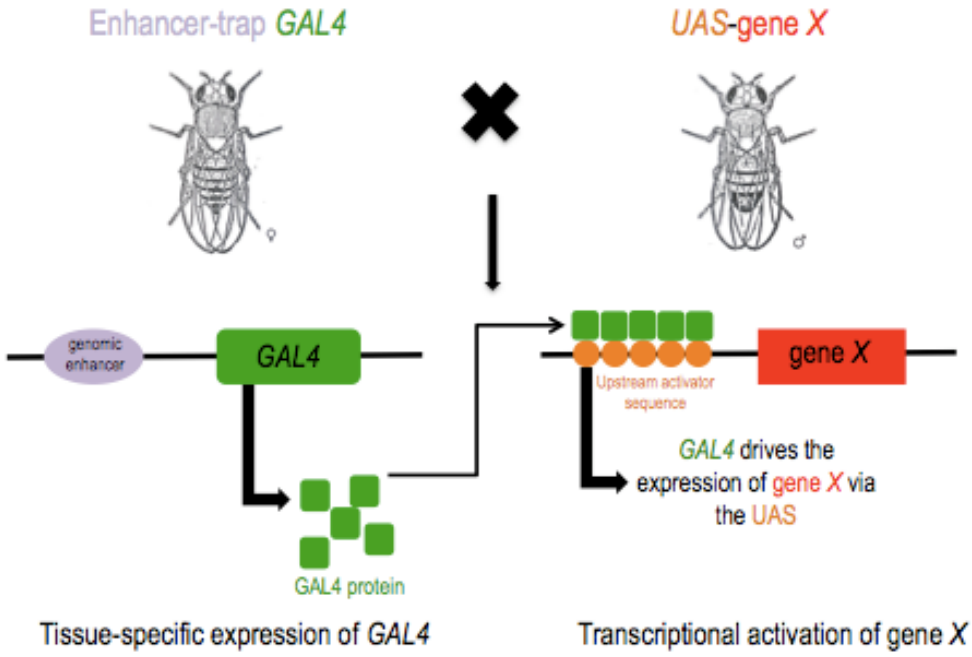

Figure 7. **The UAS/GAL4 system is used for directed gene expression.** The line on the left is the driver line and expresses GAL4 in a specific pattern. In the resulting progeny that harbor both the Gal4 driver and the UAS target, GAL4 protein then binds to the UAS, thus expressing the gene of interest in a pattern specified by the driver line used. (Figure adapted from St. Johnston, 2002).

The UAS/GAL4 system is an extremely powerful genetic tool because, due to the variety of GAL4 driver lines that exist, a gene of interest can be expressed in a variety of temporal and spatial fashions. In other words, a gene can be expressed in almost any tissue type at any time in development, depending on what driver line is used. This system is most commonly used in misexpression studies using particular genes. However, there are many other uses of this system including identification of genes involved in a specific process via enhancer- or gene-trapping, mosaic analysis, cellular marking, and analysis of loss-of-function phenotypes via targeted RNAi

expression and dominant-negative constructs (Duffy, 2002). Additionally, the UAS/GAL4 system can be used to mediate rescue experiments, such as in this study.

1.4.5 The *Drosophila* Eye Imaginal Disc

Drosophila larvae contain several imaginal discs that eventually develop into various adult structures (Figure 8). In this study, the eye/antennal disc was used for immunofluorescent staining in order to explore the roles of *alg9* and *alg10* in later stages of development in the context of the *Drosophila* visual system. The eye/antennal discs eventually develop into the adult eyes and antennae and are cupped around the larval brain.

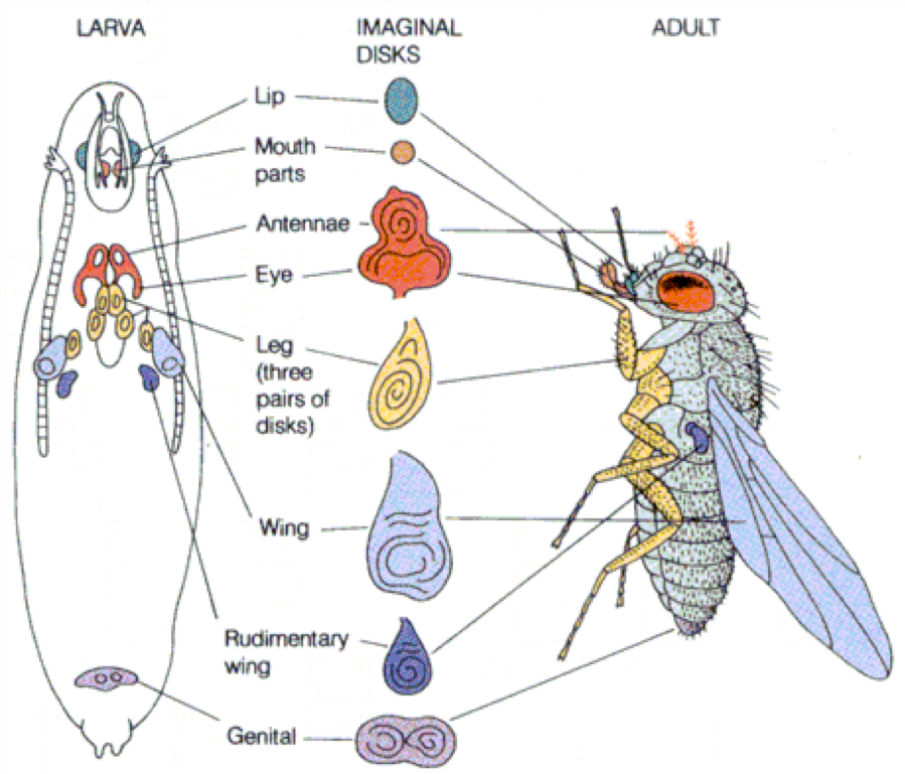

Figure 8. **Imaginal discs in *Drosophila*.** *Drosophila* larvae contain several types of imaginal discs that eventually develop into adult structures. These discs are often used to study developmental processes. The eye/antennal disc was used in this study in order to study central nervous system and photoreceptor development. (Figure adapted from Mathews and Van Holde, 1990).

The *Drosophila* eye disc is an ideal system to study eye development because photoreceptor development follows a defined sequence as the disc develops (Figure 9). The age of the disc can be easily determined, as the morphogenetic furrow moves across the disc as the eye develops and the photoreceptors differentiate behind the

furrow. This is extremely useful for observations regarding age-dependent phenotypes, such as in this study.

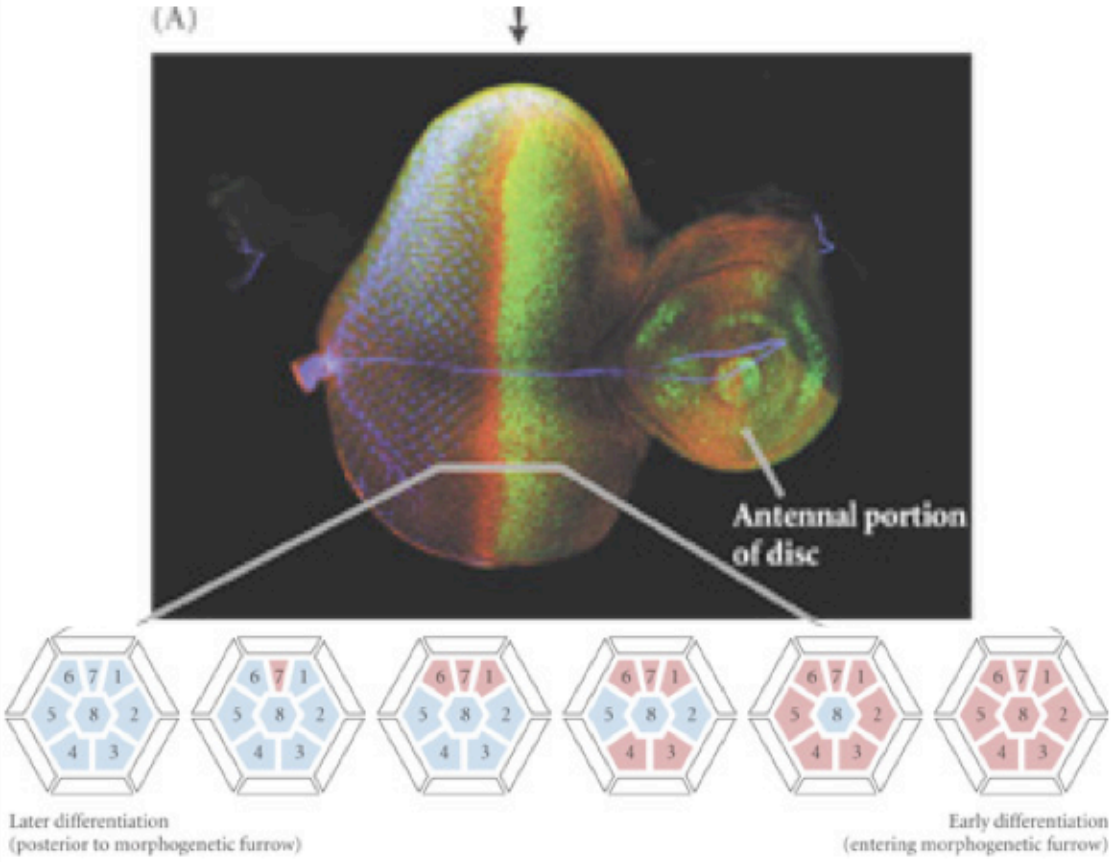

Figure 9. **The process of photoreceptor differentiation in the *Drosophila* ommatidium.** The morphogenetic furrow (arrow) moves from posterior (left) to anterior (right) along the eye disc and the photoreceptor cells differentiate in a defined sequence behind the furrow. R8 differentiates first, inducing the differentiation of R2 and R5 and the cascade then continues until R7 is differentiated. (Figure adapted from Tomlinson, 1988).

1.5 Specific Aims

The ultimate goal of this research is to extensively study and understand the role of *alg9,* acting upstream of *alg5,* compared with *alg10,* acting downstream of *alg5,* in N-linked glycosylation during development in order to reveal whether the terminal glucose added by Alg10 has a unique function in the maturation of glycosylated proteins. The specific aims of this project are:

Specific Aim 1: To characterize the embryonic phenotype of *alg10* via its effects on known glycoproteins, such as Wg and its effects on nervous system development.

Specific Aim 2: Compare the *alg10* phenotype to *alg9*, acting five steps earlier in the N-linked glycosylation.

Specific Aim 3: Examine the role of *alg9* and *alg10* during eye development by creating eye knockout models of *alg9* and *alg10*.

Specific Aim 4: Show that expression of Alg10 rescues the *alg10* mutant phenotype, using the eye knockout model.

Chapter 2

MATERIALS AND METHODS

2.1 General *Drosophila* Protocols

Fly stocks were kept in vials or bottles of prepared food media (agar, yeast, sugar, and cornmeal), Carolina™ Blue Food and yeast at 25ºC in mild humidity. Stocks were maintained by flipping flies into fresh vials or bottles every week to ten days. Offspring from experimental crosses where virgin females were being collected were kept at 18°C; collection of virgin females was performed twice a day. Males could be selected to cross to virgin females any time between adult days two and ten. Experimental crosses were expanded by flipping flies into fresh vials every four days. Collections and observations of flies were performed by anesthetizing flies using a CO_2 gun and keeping them anesthetized using a pad that releases CO_2.

2.2 Germline Clone Embryos

In order to characterize the *alg9* and *alg10* phenotypes, the *ovoD* method (see section 1.4.3.1) was used to create germline clone eggs that carried either the *alg9* or *alg10* mutation. Generation of germline clone mutant embryos via the use of this technique allows for the analysis of the effects of *alg9* and *alg10* during early stages of development without the concern of the effect of the maternal load. For a full description of the crosses used to generate germline clone mutant embryos in this study, see Appendix C. These eggs were then fertilized by males which contributed sperm carrying the corresponding mutation or sperm carrying a balancer, yielding a

mixed population of fully mutant and paternally rescued embryos that lack both the maternal and zygotic genes under study. These embryos were used for both cuticle preparations and immmunofluorescent staining for model glycoproteins and central nervous system markers. For *alg9* embryos, the marker used was *twist-GF*P and for *alg10* embryos, the marker used was *ftz-lacZ*. Fully mutant embryos were identified in immunofluorescent staining by absence of the marker. Fully mutant embryos were identified in cuticle preparations by a less severe phenotype.

2.2.1 Embryo Collection Protocol

All embryos were collected on 30-mm Petri dishes containing apple juice agar, which was made in the following manner: 750 mL of distilled water was combined with 25 grams of agar and autoclaved in a two-liter flask for a 20-minute liquid sterilization cycle. While the agar was being autoclaved, 25 grams sucrose was dissolved in 250 mL apple juice. The apple juice solution was added to the agar immediately after it was removed from the autoclave. The solution was allowed to cool to approximately 60°C, at which time 1.5 grams of Tegosept antifungal was dissolved in 10 mL of 100% ethanol was added. Plates were then filled about halfway, flamed briefly with a Bunsen burner, the agar medium was allowed to solidify, and the plates were stored at 4°C. Finely ground yeast, made using a blender, and water were combined to make a yeast paste, which was added to each plate as a food supply using a syringe. Crosses were set up and kept in collection containers on the agar plates at 25˚C and embryos were deposited in the paste and on the surrounding agar.

2.2.2 Cuticle Preparations

Embryos 24 to 48 hours in age were collected and placed at room temperature for 24 hours. Embryos were removed from the agar plate using diH_20 and a paintbrush to dislodge the embryos from the agar. The embryos were collected using a thin mesh on a collection cup. The embryos were placed in 50% bleach for 5 minutes, which dissolves the outer chorion. Embryos were rinsed thoroughly with diH_20 and placed in a microfuge tube containing one part heptane and one part methanol. The tube was vortexed for one minute in order to devitellinize the embryos. Embryos that settled to the bottom of the tube were considered devitellinized and those that remained at the interface were removed along with the heptane (top) layer. Devitellinized embryos were washed three times in methanol, rinsed four times in 1X PBT, then washed four times for 5 minutes in 1X PBT (see Appendix B). The PBT was removed and 50 mL of Hoyer's solution (see Appendix B) was added and gently mixed using a pipette tip. The embryos were allowed to equilibrate for 15 minutes before being pipetted onto a glass Fisherbrand® microscope slide and covered with a 2µm Fisherbrand® Microscope Cover Glass. Slides were kept overnight on a 55^{o}C warmer to allow the Hoyer's solution to digest the tissues inside the cuticle. After allowing the slides to cool, they were visualized using dark field on the Zeiss axiophot and images were captured.

2.2.3 General Antibody Staining Protocol for Whole Mount Embryos

Embryos 0 to 16 hours of age were collected, dechorionated, and rinsed as described in section 2.3.3. Embryos were placed in a microfuge tube containing one part 4% formaldehyde in PEM-FA (see Appendix B) and one part heptane and shaken vigorously for 20 minutes in order to be fixed. The aqueous (bottom) layer of PEM-

FA was removed using a Pasteur pipette and discarded. An equal volume of methanol was added to the top layer. After making sure there were still two layers, embryos were devitellinzied and washed in methanol as described in section 2.3.3. When only one layer was observed, more heptane was added before proceeding. At that point, embryos could be stored at -20^{o}C for up to a year or longer.

Embryos for immunofluorescent staining, were removed from the -20^{o}C and rinsed four times and washed four times for 5 minutes in PBT at room temperature. Embryos were treated with a blocking solution of PBT with 5% Normal Horse Serum (PBTN) (see Appendix B) for 30 minutes on a rocker at room temperature. Embryos were incubated in various primary antibodies at antibody-dependent dilutions (see Appendix A) in PBTN for 2 hours at room temperature or overnight at 4^{o}C. Embryos were again rinsed four times and washed four times for 5 minutes in PBT and incubated in Alexa Fluors® (Molecular Probes) secondary antibody at 1:500 (unless otherwise indicated – see Appendix A) dilution in PBTN for 1 hour at room temperature. Rinses and washes in PBT were repeated one more time before the PBT was removed and replaced with 50 μL of 70% glycerol in PBS. Embryos were allowed to equilibrate in glycerol overnight at 4^{o}C. Once all embryos had settled to the bottom, they were mounted on a glass microscope slide, covered in a glass cover slip, and sealed with nailpolish. Slides were viewed under a Zeiss LSM 780 confocal microscope and images were captured using the Zen software.

2.3 Methods for Experiments on *Drosophila* Eye Imaginal Discs

2.3.1 Generating Mosaics using the eyFlp method

The eyFlp method allows for the simple and efficient production of mitotic clones with homozygous mutant tissue exclusively in the visual system. In order to restrict recombination exclusively to the visual system, the FLP/FRT system (described in section 1.4.3) is utilized, whereby *FLP* is placed under transcriptional control of an eye-specific enhancer of the *eyeless* (*ey*) gene (Figure 10). Expression begins at around stage 15 of embryonic development when the visual system begins to develop, and is maintained until the final divisions of the eye/antennal disc in the third instar larva, ensuring homozygous mutant discs and eventually, adult eyes (Newsome, Åsling, & Dickson, 2000).

In order to eliminate all photoreceptor cells not homozygous for *alg9* or *alg10* interest, the dominant cell lethal transgene GMR-*hid* is inserted onto the chromosome arm homologous for the mutation of interest. Thus, after recombination at FRT sites, only cells containing two copies of *alg9* or *alg10* are viable (Figure 10) (Stowers and Schwarz, 1999).

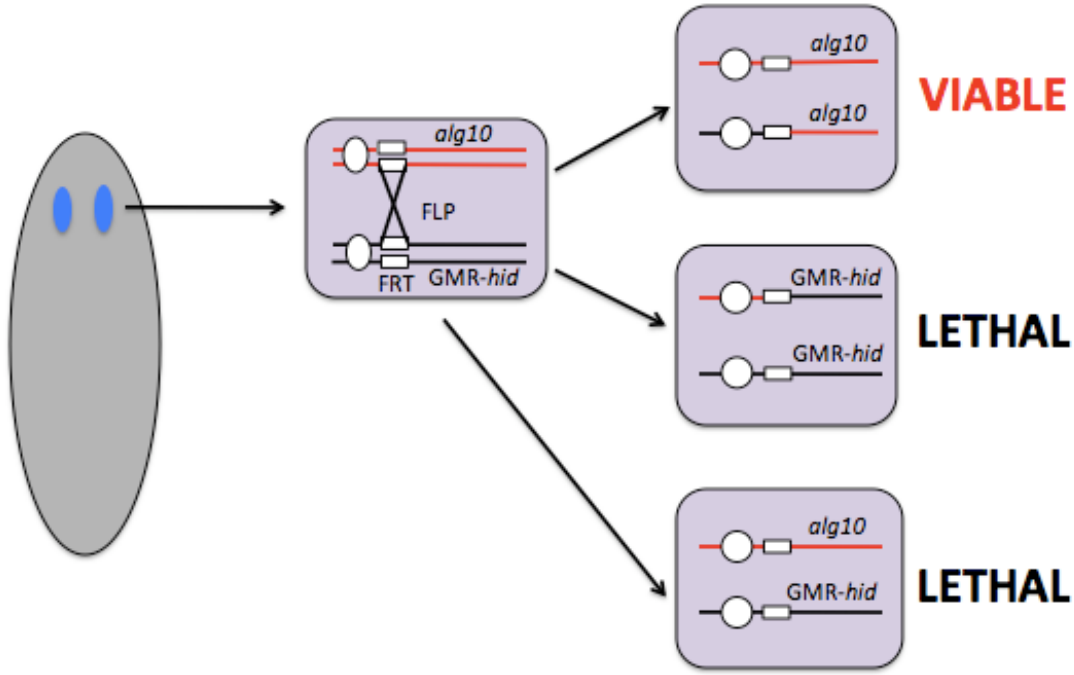

Figure 10. **Generating mosaic clones using the *eyFlp* method.** FLP recombinase is expressed in the developing eye and placed under transcriptional control of an eye-specific enhances of the *eyeless* (*ey*) gene, thereby creating mitotic clones with homozygous tissue exclusively in the developing eye. (Figure adapted from Newsome, Åsling, & Dickson, 2000).

2.3.2 Larval Collection and Dissection Protocol

In order to examine the effects of *alg9* and *alg10* on the developing eye, eye imaginal discs were isolated from third instar larvae utilizing the system depicted in Figure 10 generated using the crosses depicted in Appendix C. After three days, experimental crosses were transferred to a new vial.

Once third instar larvae began to crawl up the sides of the vial (after homologous recombination), they were harvested for primary dissection. Non-Tb larvae of the correct genotype were distinguished from Tb larvae in order to ensure

that homozygous mutant eye discs were stained. Primary dissection was performed in 1X Phosphate Buffered Saline. Primary dissection was performed by grasping larvae about the middle with one set of tweezers while using another set of tweezers to grasp the mouth hook at the anterior end of the larvae and pulling, thus removing the entire brain, including attached eye discs.

2.3.3 Larval Immunofluorescent Staining

After dissection, larval brains were fixed in 1X PBS with 4% formaldehyde for 20 minutes at room temperature. After fixation, larval brains were rinsed four times and then washed four times for 5 minutes in PBT at room temperature and blocked in PBT with 5% Normal Horse Serum (NHS) for 30 minutes at room temperature. The larval brains were incubated in various primary antibodies at antibody dependent dilutions in PBTN for 2 hours at room temperature or overnight at 4^{o}C. Antibodies used were against various central nervous system markers, markers of apoptosis, and compartment markers. Following primary incubation, larval brains were rinsed and washed four times in PBT and incubated in Alexa Fluors® from Molecular Probes secondary antibody at 1:500 dilution in PBTN for 1 hour at room temperature. Larval brains were rinsed and washed four more times before secondary dissection.

Secondary dissection was performed in PBT. Secondary dissection involved carefully separating the eye discs from the lobes of the larval brain using tweezers and isolating the discs for mounting. Dissected eye discs were mounted on a microscope slide in 70% glycerol in PBS, covered with a cover slip, and sealed with nail polish. Stained eye discs were then visualized with a Zeiss LSM 780 confocal microscope and images were captured using the Zen software.

2.4 Methods for Experiments on Adult *Drosophila* Eyes

A rescue experiment was performed for *alg10* using the UAS/GAL4 system described in section 1.4.4. The *alg10* mutant phenotype in adult eyes was rescued by crossing virgin females that were *UASalg10/(CyO); alg10-10FRT/TM6C* with males that were *UASFlpeygal4/SM5; gmrhidFRT/TM6B*. By using eygal4 as the driver, gene expression of *alg10* was directed specifically to the eye tissue. Crosses used to obtain non-Sb adults displaying the rough eye phenotype as well as adult rescue eyes (Figure 18) can be found in Appendix C. All images in Figure 18 were taken using a camera attached to a dissection microscope. All images in Figure 17 were taken using scanning electron microscopy. Processing for sectioning was done at Delaware Biotechnology Institute, based on the protocol of Gaengel and Mlodzik (2008).

2.4.1 Preparing Adult Heads for Sectioning

Flies of the appropriate genotype (see Appendix C) were decapitated using tweezers. A small section of one eye was then cut using a scalpel; the rest of the head was then placed in 2% glutaraldehyde in PBS at 4^{O}C and held in fixative until further processing.

2.4.2 Processing of Adult Heads for Sectioning

Heads were fixed in 1% glutaraldehyde and 1% osmium tetroxide in Sorensen's phosphate buffer pH 7.2 for one hour on ice, then 2% osmium tetroxide in 0.1M Sorensen's phosphate buffer pH 7.2 for one hour on ice. Heads were dehydrated via the following ascending ethanol series: 30%, 50%, 70%, 90%, anhydrous 100%; each was done for 10 minutes on ice. Heads were dehydrated again for 10 minutes in

100% anhydrous ethanol at room temperature and the ethanol was replaced with propylene oxide 2 times for 10 min, each at room temperature.

2.4.3 Embedding Adult Heads

Eyes were infiltrated using Embed-812 resin at room temperature in the following sequence: 1 part resin: 3 parts propylene oxide for 2 hours, 1 part resin: 2 parts propylene oxide overnight, 1 part resin: 1 part propylene oxide for 2 hours, 2 parts resin: 1 part propylene oxide for 2 hours, 3 parts resin: 1 part propylene oxide overnight, 100% resin for 2 hours, 100% resin overnight. Heads were then embedded in flat embedding molds and polymerized at 60^{O}C for 24 hours.

2.4.4 Sectioning and Staining Adult Eyes

Eyes were sectioned with a Reichert-Jung UltraCut E ultramicrotome using a Diatome Histo Jumbo diamond knife. Semi-thick sections (0.5 μm) were collected onto Superfrost® Plus microscope slides and stained with 1% toluidine blue and 1% borax in double distilled water on a hotplate. Slides were rinsed with double-distilled water, air dried, and mounted in DPX mountant with 22 x 40 mm, No. 1.5 cover glass.

Chapter 3

RESULTS

3.1 Both *alg9* and *alg10* Show Severe Cuticle Defects

Cuticle preparations were performed on fully mutant as well as paternally rescued *alg9* and *alg10* germline clone embryos generated via the *ovoD* method (described in section 2.3.1) in order to characterize the *alg9* and *alg10* phenotypes (Figure 11). The wild type showed normal cuticle secretion in defined denticle bands. Paternally rescued *alg9* and *alg10* embryos showed abnormal secretion of cuticle, displaying denticle lawns or absent/interrupted bands. Fully mutant *alg9* and *alg10* embryos showed very little to almost no cuticle secretion and a severely disfigured body shape. These phenotypes are indicative of severe defects early in embryogenesis.

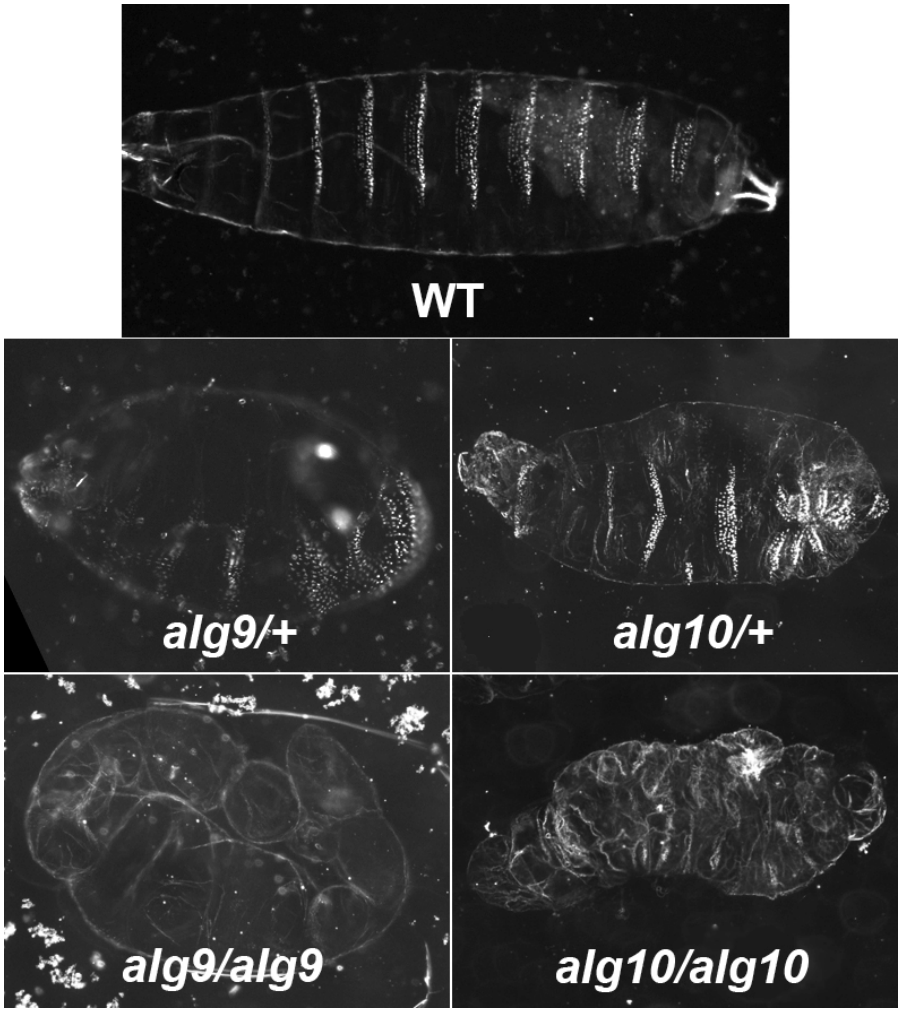

Figure 11. **Cuticle images of *alg9* and *alg10* germline clone embryos.** Both fully mutant *alg9* (bottom left) and *alg10* (bottom right) embryos lack cuticle and show a disfigured body shape. Paternally rescued *alg9* (middle left) and *alg10* (middle right) show abnormal secretion of cuticle compared to the wild type (top).

3.2 *alg9* and *alg10* Show Defects in Wg Secretion

When immunoflorescent staining of Wg, a model secreted glycoprotein of the Wnt pathway, was performed on fully mutant and paternally rescued *alg9* and *alg10* germline clone embryos, both *alg9* and *alg10* paternally rescued embryos showed Wg

punctated vesicles outside of expressing cells, indicative of Wg secretion. These punctates were absent in fully mutant *alg9* and *alg10* embryos and Wg accumulated in expressing cells (Figure 12).

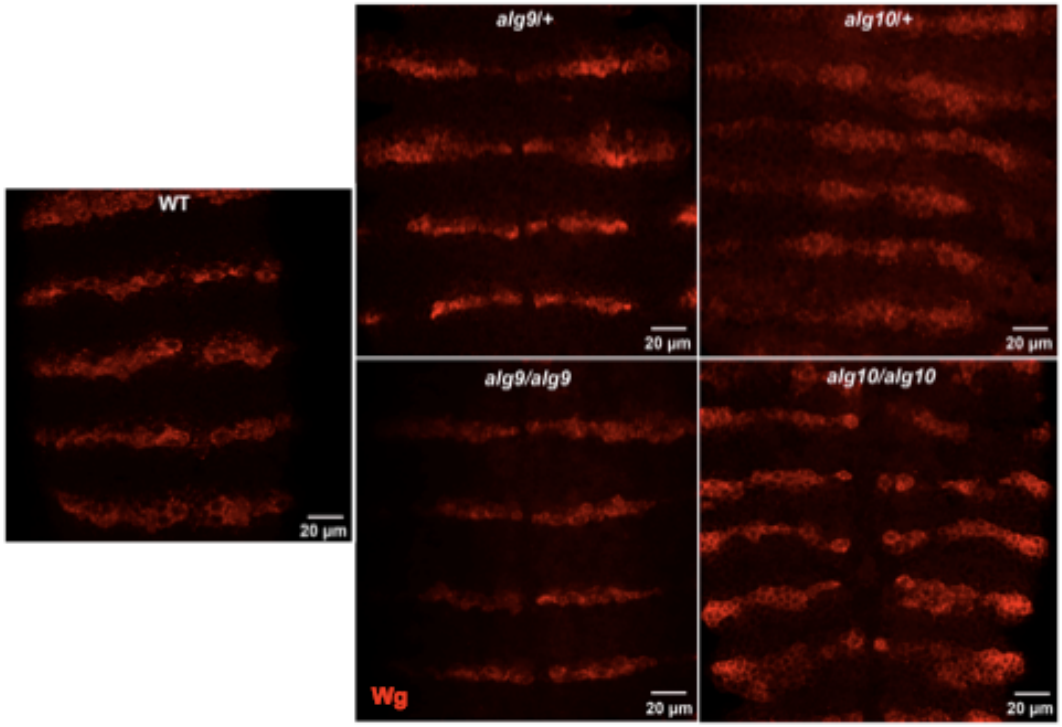

Figure 12. ***alg9* and *alg10* show defects in Wg secretion.** WT (left) and paternally rescued *alg9* and *alg10* embryos (top) show Wg punctuated vesicles, while fully mutant *alg9* and *alg10* embryos (bottom) lack these punctates. Paternal rescue was recognized by the presence of the balancer chromosome *twist-GFP* (*alg9*) or *ftz-lacZ* (*alg10*), stained in green (not shown).

3.3 *alg9* and *alg10* Do Not Affect Downstream Wg Signaling

Immunofluorescent staining of Engrailed (En), a downstream target of Wg in the developing embryo, was performed on fully mutant germline clone embryos. The

presence of En staining in both *alg9* and *alg10* mutant embryos indicates that Wg signaling may have been impaired, but it was not absent (Figure 13).

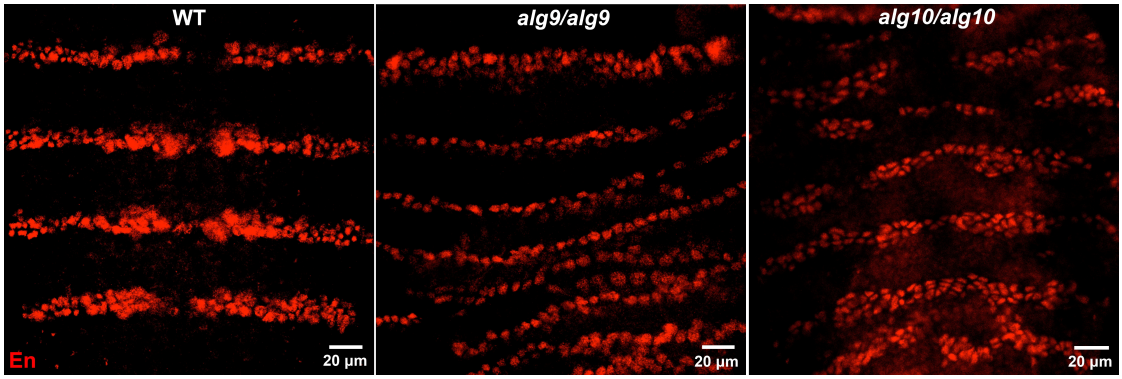

Figure 13. **Both *alg9* and *alg10* show signaling downstream of Wg.** Non-paternal rescue was recognized by the absence of the balancer chromosome *twist-GFP* (*alg9*) or *ftz-lacZ* (*alg10*) stained in green (not shown).

3.4 Non-Paternally Rescued *alg9* Lacks a Developed Central Nervous System

Because it is well established that N-linked glycosylation is important for neuronal development, potential nervous system defects were explored in both *alg9* and *alg10* germline clone embryos. To this end, expression of 22C10, required for dendritic and axonal development in the central nervous system (CNS) (Hummel et al., 2000), and ELAV, required for correct differentiation and maintenance of the nervous system (Berger et al., 2007), was observed in non-paternally rescued *alg9* and *alg10* germline clone embryos (Figure 14). While ELAV and 22C10 positive *alg10* embryos were present at stage 13, these markers could only be found at the start of CNS development in stage 9 *alg9* embryos. This finding implies that non-paternally rescued *alg9* embryos lacked a developed central nervous system, while *alg10* showed severe CNS defects.

Similar results were observed in a staining of the CNS axons of *alg9* and *alg10* germline embryos at stage 13 using BP102, an axonal marker, with ELAV (Figure 15). The BP102 CNS axon marker was never detected in *alg9* embryos, once again supporting the conclusion that non-paternally rescued *alg9* embryos lacked a developed central nervous system.

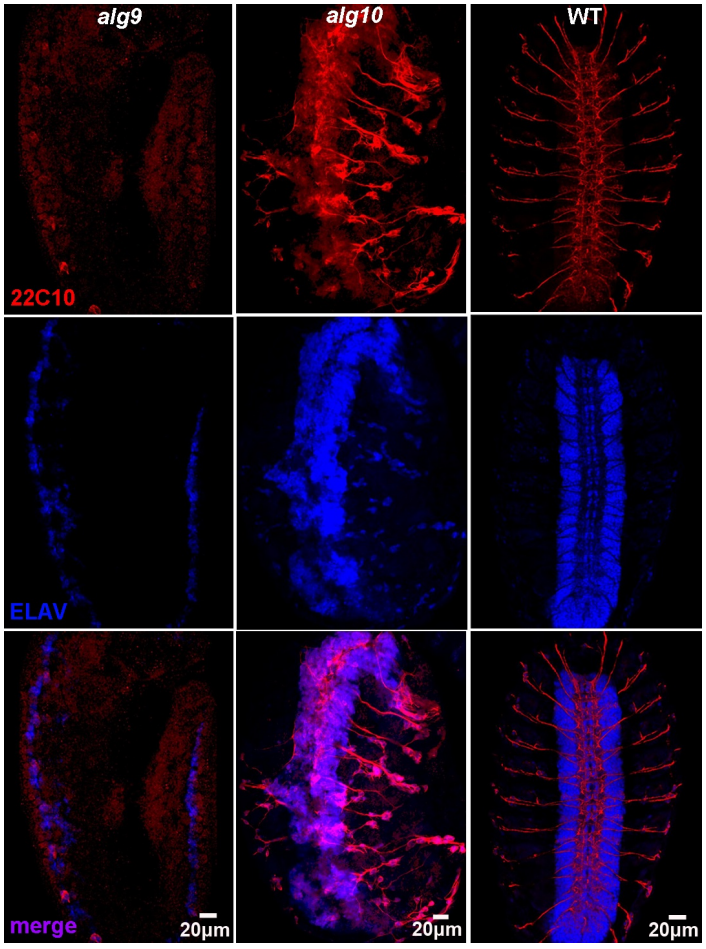

Figure 14. **Fully mutant *alg9* lacks a fully developed CNS and fully mutant *alg10* shows severe CNS defects.** Expression of 22C10 (red), a dendritic marker and ELAV (blue), a pan-neuronal marker, in non-paternally rescued *alg9* (left, stage 9) and *alg10* (middle, stage 13) germline clone embryos. Non-paternal rescue was recognized as in Figure 13.

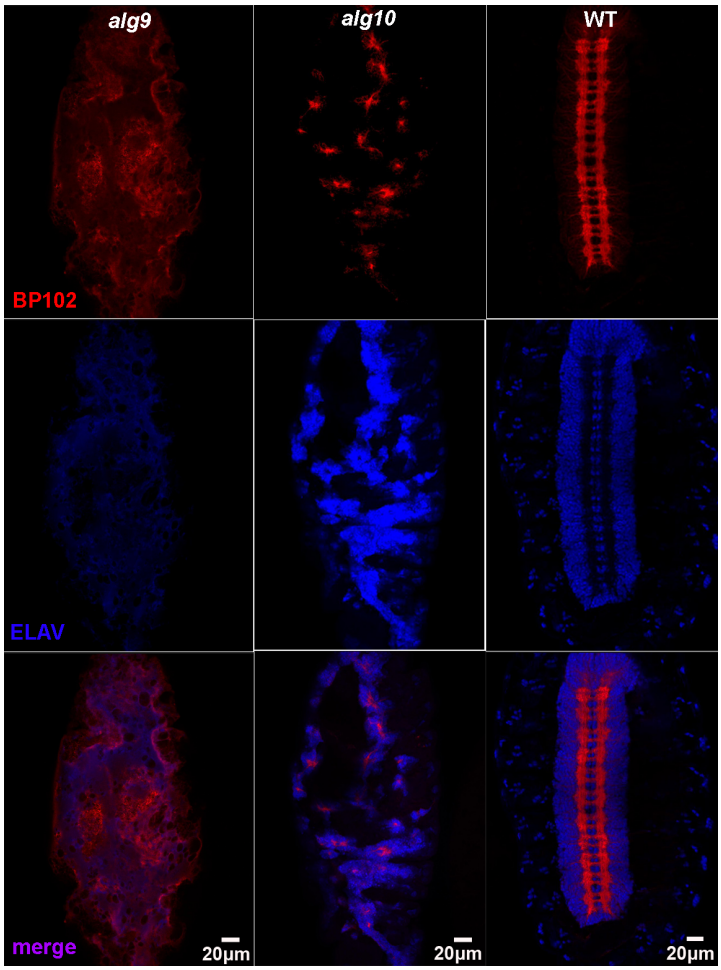

Figure 15. **Fully mutant *alg9* lacks a fully developed CNS and fully mutant *alg10* shows severe CNS defects.** Expression of BP102 (red), an axonal marker, and ELAV (blue), a pan-neuronal marker, in non-paternally rescued *alg9* (left) and *alg10* (middle) stage 13 germline clone embryos. Non-paternal rescue was recognized as in Figure 13.

3.5 *alg9* and *alg10* Show Commitment to Pro-neuronal Cell Fates

Once it was observed that fully mutant *alg9* embryos lacked a developed CNS, the question was whether this was because the cells never differentiated or because they differentiated and then failed to become fully mature neurons. In order to address

this question, a staining for achaete (ac), a neuroblast marker, was performed. Neuroblast specification in *alg9* germline clone embryos at stage 9 was similar to the wild type, indicating neurons in this background were specified, but failed to become mature neurons by stage 13 (Figure 16).

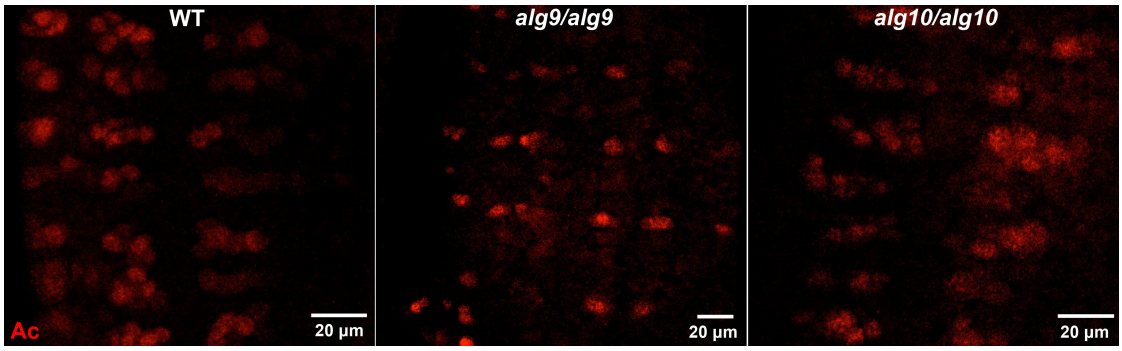

Figure 16. ***alg9* Germline Clone Embryos Show Acheate Staining, Indicating Specification.** Expression of achaete, a neuroblast marker, in *alg9* (stage 9) and *alg10* (stage 7) embryos. Non-paternal rescue identified as in Figure 4.

3.6 Adult *alg9* and *alg10* Eyes Show a Rough Eye Phenotype and the *alg10* Phenotype is Rescued in the Presence of Alg10

Compared to the wild type, adult eyes lacking *alg10* showed a rough eye phenotype with a smaller eye size (Figure 17). This phenotype was intermediate of that of the WT and that of GMR-*hid*, the stock necessary to generate adults with homozygous mutant eyes. The *hid* gene encodes a proapoptotic protein that induces complete photoreceptor lethality. The fact that the *alg10* phenotype was similar to the GMR-*hid* phenotype, but less severe, indicates that photoreceptors in *alg10* eyes may have died by apoptosis.

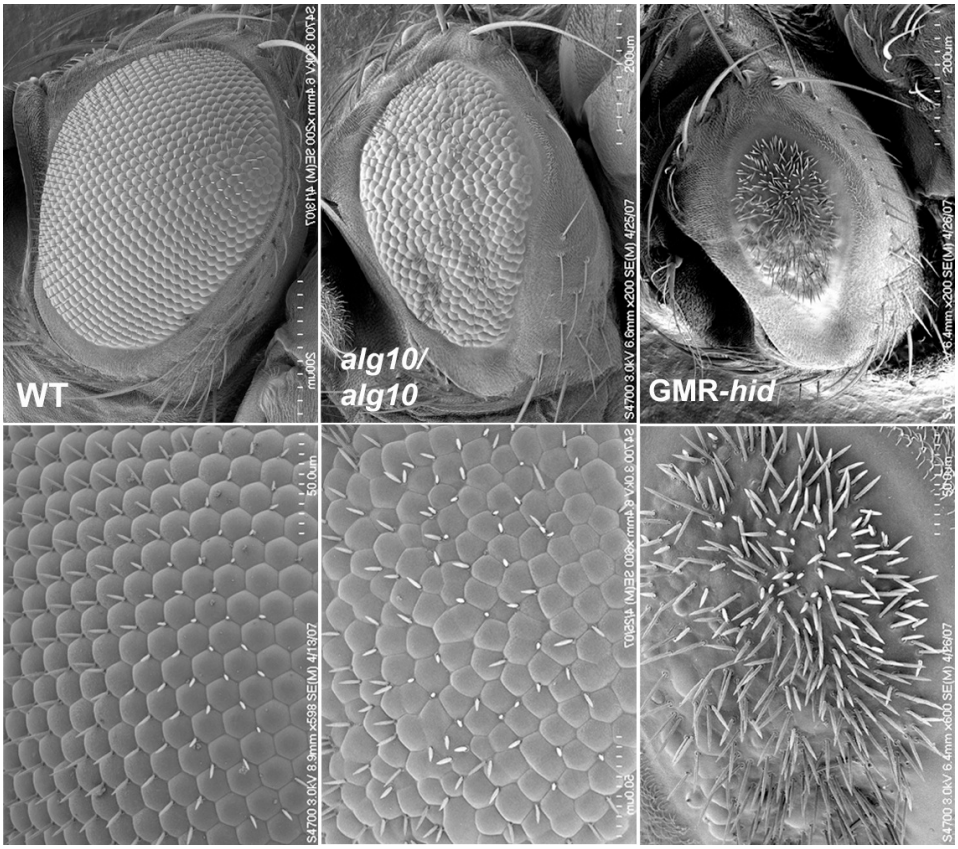

Figure 17. **Adult *alg10* eyes show a rough eye phenotype.** Scanning electron micrograph of WT (left), *alg10* (middle), and GMR-*hid* (right) adult eyes. *alg10* adult eyes show a rough eye phenotype, intermediate of that of the WT and that of GMR-*hid*, the stock necessary to generate adults with homozygous mutant eyes. *hid* induces complete photoreceptor lethality.

Adult *alg9* eyes also showed a rough eye phenotype with a smaller eye size (Figure 18). This phenotype was more severe than the *alg10* phenotype, consistent with observations in the embryo. Additionally, the rough eye phenotype observed in *alg10* was rescued when *UAS-alg10* was expressed in the eye using *eygal4*, as

described in section 2.2.4. Rescue confirms that the loss of *alg10* was the cause of the rough eye phenotype.

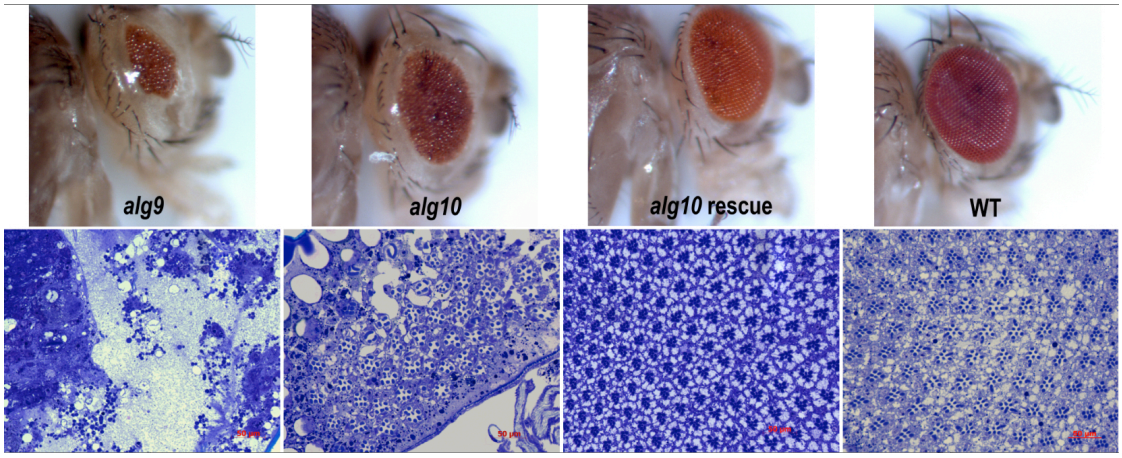

Figure 18. **Adult *alg9* eyes also show a rough eye phenotype and the *alg10* phenotype is rescued in the presence of Alg10.** Images taken of *alg9* (far left), *alg10* (center left), *alg10* rescue (center right), and WT (far right) adult eyes using a dissection microscope. Bottom: Light microscope images of toluidine blue stained plastic sections of adult eyes of the same genotypes. The *alg10* rescue flies show an eye phenotype similar to that of the WT, indicating that *alg10* phenotype is rescued in the presence of Alg10.

3.7 Developing *alg9* and *alg10* Eyes Show Defects in Axon Pathfinding

In order to explore the potential source of this rough eye phenotype in the adults, eye discs were isolated from 3rd instar larvae and stained for chaoptin, a surface glycoprotein on axons, and caspase, an indicator or apoptosis (Luong et al. 2013). In earlier stage eye discs, *alg9* and *alg10* developing eyes showed disrupted axon tracks leading from the photoreceptors to the brain (Figure 19); however, apoptosis at this stage was not yet significant, indicating that this defect was not simply due to cell death. Both *alg9* and *alg10* also caused retention of chaoptin in the cell bodies, possibly due to its improper glycosylation.

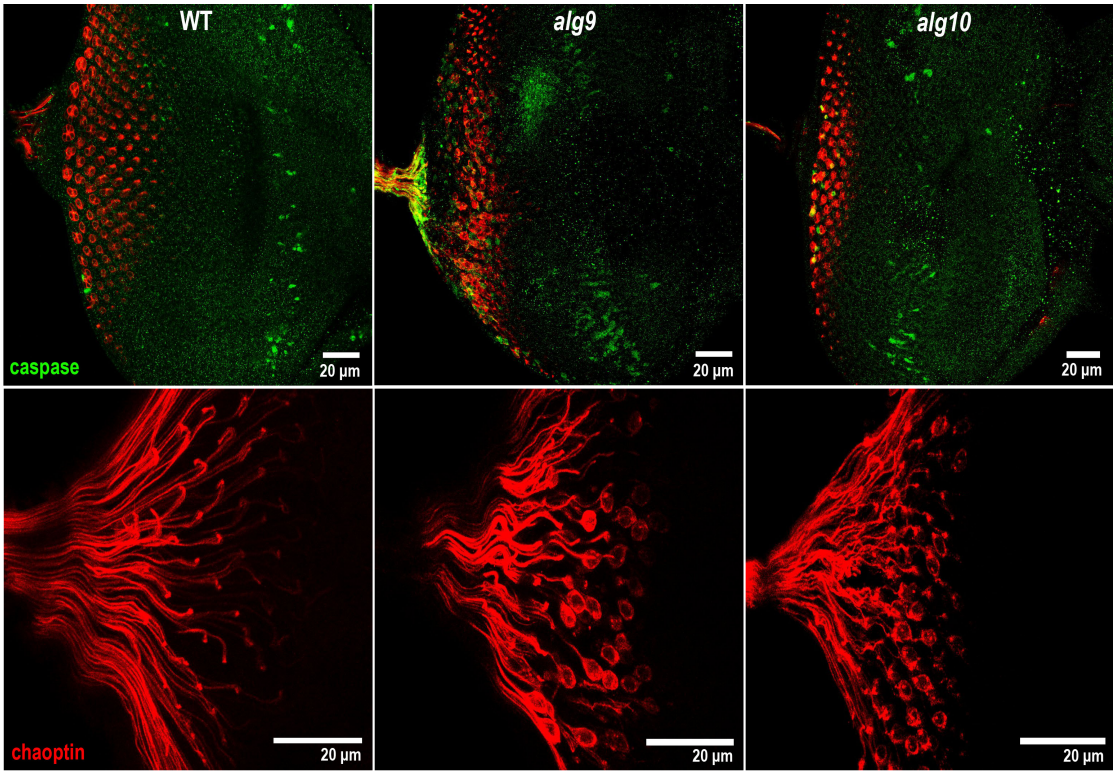

Figure 19. **Developing *alg9* and *alg10* eyes show defects in axon pathfinding.** Expression of chaoptin (red), a surface glycoprotein on axons and caspase (green), an indicator of apoptosis, in eye imaginal discs from 3rd instar larvae at both 40x (top) and 100x (bottom). Both *alg9* and *alg10* developing eyes show disrupted axon tracks leading from photoreceptors to the brain early in eye development, yet apoptosis at this stage is not significant.

Later in eye development, Bolwig's nerve was observed in the WT developing eye, but not in *alg9* or *alg10* developing eyes, which is further indicative of defects in axon pathfinding (Figure 20). Additionally, both *alg9* and *alg10* developing eyes displayed massive apoptosis in older cells, indicating that neurons began to die after specification due to the absence of appropriate glycoproteins. This massive and age-

dependent photoreceptor death may be the cause of the rough eye phenotype in the adults.

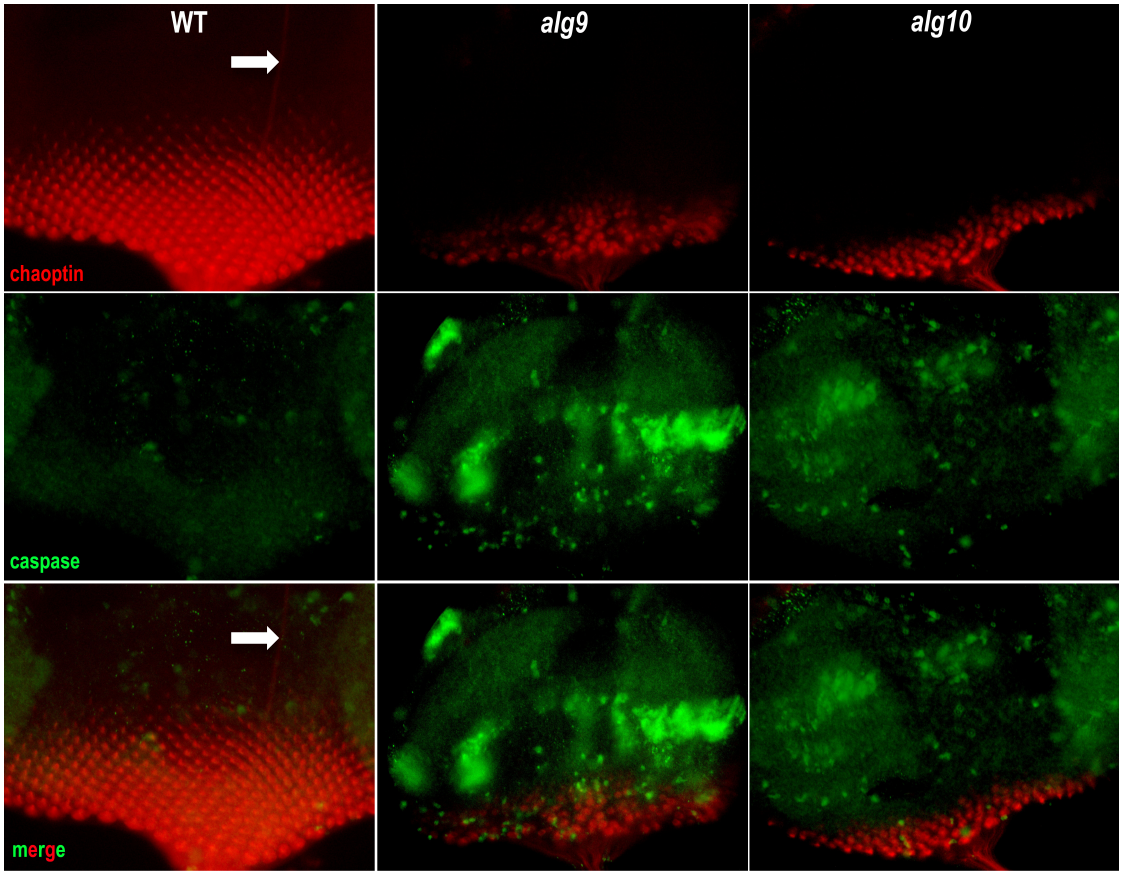

Figure 20. **Developing *alg9* and *alg10* eyes lack Bolwig's nerve.** Expression of chaoptin (red) and caspase (green) in in eye imaginal discs from 3rd instar larvae. While Bolwig's nerve (white arrow) can be observed in the WT developing eye (left), it is absent in both *alg9* (middle) and *alg10* developing eyes (right). Additionally, both *alg9* and *alg10* developing eyes display massive apoptosis in older cells.

Chapter 4

DISCUSSION

Recent advances in the understanding of the *Drosophila* glycome make it the perfect model organism to study N-linked glycosylation. Due to the fact that both the A and the B isoforms of oligosaccharyltransferase are known to exist in *Drosophila*, I hypothesized that loss of *alg9* would be more severe than the absence of *alg10*; interrupting N-glycosylation upstream of *alg5* would produce proteins that were not glycosylated, whereas interrupting N-glycosylation downstream of *alg5* would perhaps create proteins that were underglycosylated. Interrupting N-glycosylation downstream of *alg5* may also only affect a subset of glycoproteins. By comparing the phenotypes of *alg9* and *alg10* mutants, it was possible to glean insight into the role that the terminal glucose added by Alg10 plays in *Drosophila* development.

I began this study by characterizing the *alg9* and *alg10* phenotypes using germline clone embryos, both for cuticle preparations and immunofluorescent staining. The cuticle preparation showed that loss of both *alg9* and *alg10* caused severe and pleiotropic cuticle defects (Figure 11). The abnormal secretion of cuticle (missing bands, interrupted bands, bands that are not well-defined) in paternally rescued *alg9* and *alg10* embryos indicates that some of the defects were consistent with loss of Wg or Hh signaling, which are essential for the normal secretion of naked cuticle in developing embryos (Wharton Jr. et al., 2001). Because of the observed cuticle defects and the fact that Wg is a glycoprotein, I examined Wg in *alg9* and *alg10* mutant embryos.

When stained for Wg, paternally rescued *alg9* and *alg10* mutants had Wg punctuated vesicles, an indication that Wg was being normally secreted, at least in part (Figure 12). However, fully mutant *alg9* and *alg10* did not have punctates, suggesting Wg signaling was impaired and thus Wg signaling was likely disrupted. However, when stained for En, a downstream target of Wg signaling, En was unexpectedly expressed in fully mutant *alg9* and *alg10* embryos, indicating that Wg secretion and signaling may be impaired, but was not absent (Figure 13). There was a patterning defect observable in fully mutant *alg9* and *alg10* embryos in the En staining. This may be something interesting to explore in the future, along with staining for other downstream targets of Wg signaling. In particular, long-range targets of Wg signaling may be more severely affected by a defect in Wg secretion caused by its improper glycosylation.

Because N-linked glycosylation has been shown to be important in many aspects of neuron development (Kleene & Schachner, 2004), it was decided to explore potential central nervous sytem defects in the germline clone embryos. The CNS markers 22C10, BP102, and ELAV were used to stain fully mutant and paternally rescued germline clone embryos (Figures 14 and 15). These experiments revealed the phenotypic difference between *alg9* and *alg10* that had been predicted. Fully mutant *alg10* embryos showed severe CNS defects at stage 13, while fully mutant *alg9* embryos failed to develop a mature CNS entirely; no *alg9* embryos were found beyond stage 9. These results support my hypothesis that *alg9* defects would be more severe than *alg10* defects. Furthermore, examining the neuroblast specification marker achaete (Skeath, 1998) confirmed that *alg9* embryos show commitment to pro-neuronal cell fates, but fail to become fully mature neurons (Figure 16).

These results warranted further exploration, so the project shifted its focus to looking at the developing *Drosophila* eye, which enabled exploring the role of glycosylation later in development in the context of the central nervous system, which is inextricably linked to the visual system. For these experiments, both eye discs from third instar larvae and adult eyes generated via the eyFlp technique were utilized. A scanning electron micrograph taken previously had shown that *alg10* adult eyes have a rough eye phenotype (Figure 17). This phenotype is intermediate of that of the WT and that of GMR-*hid*, the stock necessary to generate adults with only homozygous mutant eyes. Because *hid* induces complete photoreceptor lethality, the fact that the *alg10* phenotype was similar to the GMR-*hid* phenotype, but less severe, indicated that photoreceptors in *alg10* eyes may have died by apoptosis.

Expanding upon this work, the dissection microscope was employed to take images of both *alg9* and *alg10* adult eyes. These images confirmed that *alg10* has a rough eye phenotype, in addition to a smaller eye size (Figure 18). These images also showed that *alg9* also has a rough eye phenotype and it is more severe than the *alg10* phenotype. This result is consistent with what was observed in the embryo and again supports my hypothesis that *alg9* defects are worse than *alg10* defects. Additionally, after trying unsuccessfully in the embryo (data not shown), it was possible to carry out the rescue experiment in the adults. The rescued *alg10* adults showed marked improvement in the rough eye phenotype, with an eye size similar to that of the wild type and a similar ommatidial structure.

By using eye imaginal discs to observe developing *alg9* and *alg10* eyes, it could be shown that the rough eye phenotype observed in the adults was due to age-dependent photoreceptor death later in eye development, marked by increased caspase

expression, an indicator of apoptosis (Figure 20). Consistent with observations in the embryo, the likely explanation for this observation is that neurons are specified, but then begin to die after specification due to lack of appropriate glycoproteins. Furthermore, developing *alg9* and *alg10* eyes showed defects in axon pathfinding (Figure 19), as indicated by chaoptin, a surface glycoprotein on the axon. This phenotype is also consistent with those seen in fully mutant *alg10* embryos, as well as paternally rescued *alg9* and *alg10* embryos (data not shown).

There are many potential avenues to explore in order to take this project further. In addition to plastic sections, cryosections of adult eyes can be taken and stained with molecular markers for target glycoproteins, such as Fasciclin (Fas) and Crumbs (Crb) in order to look at their localization in the eye. These markers and many others, such as compartment markers, can also be used to stain eye discs in order to expand that data set. Furthermore, using protein extracts obtained from mutant adult fly heads obtained from this system, Western blot analysis can be performed to determine if the target glycoprotein requires the addition of the terminal glucose catalyzed by Alg10 (if it was required, we predict that the *alg* mutant extract will show a lower molecular weight for target glycoproteins relative to wild type, due to under-glycosylation. Additionally, many of the described experiments can be repeated in order to ensure a publication quality data set.

However, based on the work described in this thesis, the following conclusions can be drawn:

1.) Both *alg9* and *alg10* mutants show severe cuticle defects.

2.) Disrupting N-linked glycosylation negatively affects the secretion of the glycosylated signaling ligand Wg, but does not affect downstream Wg short-range signaling.

3.) *alg9* and *alg10* show differentiation of pro-neuronal cells; however, fully mutant *alg9* lacks mature neurons.

4.) Loss of *alg10* in the developing eye disrupts normal neuronal maturation and displays severe defects in axon pathfinding.

5.) Both *alg9* and *alg10* adult eyes show a rough eye phenotype, which is more severe in *alg9*. The *alg10* rough eye phenotype can be rescued in the presence of Alg10.

6.) Massive apoptosis during later stage eye development indicates neurons differentiate and then begin to die upon maturation, which may explain phenotypes observed in the embryo and the adult.

7.) *alg10* causes severe defects in *Drosophila* development. However, the enzyme it encodes may only be required for glycosylation of a sub-set of glycoproteins that pass through the secretory pathway as its phenotype is less severe than *alg9*, encoding an enzyme that acts five steps earlier in the N-glycosylation pathway.

REFERENCES

Berger, Christian, Renner, Simore, Lüer, Karin, & Technau, Gerhard M. (2007). The commonly used marker ELAV is transiently expressed in neuroblasts and glial cells in the *Drosophila* embryonic CNS. *Developmental Dynamics, 236*(12), 3562-3568. doi: 10.1002/dvdy.21372

Burda, P., & Aebi, M. (1999). The dolichol pathway of N-linked glycosylation. *Bichimica et Biophysica Acta, 1426*(2), 239-257.

Duffy, J. B. (2002). GAL4 system in *Drosophila*: A fly geneticist's Swiss army knife. *Genesis, 34*, 1-15. doi: 10.1002/gene.10150

Fernández-Moreno, M. A., Farr, C. L., Kaguni, L. S., & Garesse, R. (2007). *Drosophila melanogaster* as a model system to study mitochondrial biology. *Methods Mol. Biol., 372*, 33-49.

Freeze, H. H. (2006). Genetic defects in the human glycome. *Nature Reviews, 7*, 537-551. doi: 10.1038/nrg1894

Gaengel, Konstantin & Mlodzik, Marek (2008). Microscopic analysis of the adult *Drosophila* retina using semithin plastic sections. *Methods Mol. Biol., 420,* 277-287. doi: 10.1007/978-1-59745-583-1_17

Haecker, A., Bergman, M., Neupert, C., Moussain, B., Luschnig, S., Aebi, M., & Mannervik, M. (2008). Wollknäuel is required for embryo patterning and encodes the *Drosophila* ALG5 UDP-glucose:Dolichyl-phosphate glucosyltransferase. *Development, 135*, 1745-1749. doi: 10.1242/dev.020891

Haeuptle, M. A., & Hennet, T. (2009). Congenital disorders of glycosylation: An update on defects affecting the biosynthesis of dolichol-linked oligosaccharides. *Human Mutation, 30*(12), 1628-1641. doi: 10.1002/humu.21126

Hentges, K. E., & Justice, M. J. (2004). Checks and balancers: Balancer chromosomes to facilitate genome annotation. *Trends in Genetics, 20*(6), 252-259. doi: 10.1016/j.tig.2004.04.004

Hummel, Thomas, Krukkert, Karin, Roos, Jack, Davis, Graeme, & Klämbt, Christian (2000). Drosophila Futsch/22C10 Is a MAP1B-like Protein Required for Dendritic and Axonal Development. *Neuron, 26,* 357-370.

Kleene, Ralf & Schachner, Melitta (2004). Glycans and neural cell interactions. *Nature Reviews Neuroscience, 34*(4), 853-858.

Luong, Linh Ly, Suyari, Osamu, Yoshioka, Yasuhide, Tue, Nguyen Trong, Yoshida, Hideki, & Yamaguchi, Masamitsu (2013). dNF-YB plays dual roles in cell death and cell differentiation during *Drosophila* eye development. *Gene, 520*(2), 106-118. doi: http://dx.doi.org/10.1016/j.gene.2013.02.036

Mathews, C. K., & Van Holde, K. E. (1990). *Biochemistry*. Redwood City, California: Benjamin/Cummings Publishing Company.

Newsome, T. P., Åsling, B., & Dickson, B. J. (2000). Analysis of *Drosophila* photoreceptor axon guidance in eye-specific mosaics. *Development, 127*, 851-860.

Selva, E. M., & Stronach, B. E. (2007). Germline clone analysis for maternally acting *Drosophila* hedgehog components. *Methods in Molecular Biology: Hedgehog Signaling Protocols, 397*, 129-144. doi: 10.1007/978-1-59745-516-9_11

Shaik, K. S., Pabst, M., Schwarz, H., Altmann, F., & Moussian, B. (2011). The Alg5 ortholog wollknäuel is essential for correct epidermal differentiation during *drosophila* late embryogenesis. *Glycobiology, 21*(6), 743-756. doi: doi:10.1093/glycob/cwq213

Shrimal, Shiteshu, Trueman, Steven F., & Gilmore, Reid (2013). Extreme C-terminal sites are posttranslocationally glycosylated by the STT3B isoform of the OST. *J. Cell Biol., 201*(1), 81-95. doi: 10.1083/jcb.201301031

Skeath, James B. (1998). The *Drosophila* EGF receptor controls the formation and specification of neuroblasts along the dorsal-ventral axis of the *Drosophila* embryo. *Development, 125,* 3301-3312.

St. Johnston, D. (2002). The art and design of genetic screens: *Drosophila melanogaster*. *Nature Reviews Genetics, 3*, 176-188. doi: 10.1038/nrg751

Stephenson, R. & Metcalfe, N. (2013). *Drosophila melanogaster*: A fly through its history and current use. *J R Coll Physicians Edinb, 43*, 70-75. doi: http://dx.doi.org/10.4997/JRCPE.2013.116

Stowers, R. Steven & Schwarz, Thomas L. (1999). A Genetic Method for Generating Drosophila Eyes Composed Exclusively of Mitotic Clones of a Single Genotype. *Genetics, 152*, 1631-1639.

Tennessen, J. M. & Thummel, C. S. (2011). Coordinating growth and maturation - insights from *Drosophila*. *Current Biology, 21*, R750-R757. doi: 10.1016/j.cub.2011.06.033

Theodosiou, N. A. & Xu, T. (1998). Use of the FLP/FRT system to study *Drosophila* development. *A Companion to Methods in Enzymology, 14*, 355-365.

Tomlinson, A. (1988). Cellular interactions in the developing *Drosophila* eye. *Development, 104*, 183-193.

Wharton Jr., Keith A., Zimmerman, Gregor, Rousset, Raphaël, & Scott, Matthew P. (2001). Vertebrate Proteins Related to *Drosophila* Naked Cuticle Bind Dishevelled and Antagonize Wnt Signaling. *Developmental Biology, 234,* 93-106. doi: 10.1006/dbio.2001.0238

Appendix A

ANTIBODIES

Antibodies against a variety of markers at a variety of dilutions were used to stain germline clone embryos and eye imaginal discs. All antibodies were stored at 4^{o}C. When being used more than once, primary antibodies were stored in PBTN at the correct dilution with 0.1% sodium azide (NaN_3). Secondary antibodies were all Alexa Fluor® Dyes (Life Technologies) that allowed the markers to be visualized at specific excitable wavelengths via fluorescence excitation under a confocal microscope. A comprehensive list of the primary and secondary antibodies used in experiments in this study and their targets is detailed in the following Tables:

Primary Antibody	Abbreviation	Dilution	Marker
Rabbit Anti-β-Galactosidase	Rbαβgal	1:100	Hydrolase Enzyme
Chicken Anti-β-Galactosidase	Chkαβgal	1:100	Hydrolase Enzyme
Mouse Anti-Wingless	MαWg	1:10	Wingless Signaling Molecule
Rat Anti-ELAV	RαELAV	1:20	Pan-Neuronal Cell Body
Mouse Anti-BP102	MαBP102	1:10	CNS Axonal Marker
Mouse Anti-22C10	Mα22C10	1:10	CNS Dendritic Marker
Mouse Anti-FasciclinIII	MαFasIII	1:10	CNS Neurons and Axons
Mouse Anti-Achaete	MαAc	1:4	Neuroblast Marker
Mouse Anti-Engrailed	MαEn	1:4	Downstream Target of Wingless
Mouse Anti-Crumbs	MαCrb	1:10	Cell Polarity
Rat Anti-E-cadherin	RαE-cad	1:10	Epithelial Junction Protein
Rabbit Anti-GM130	RbαGM130	1:100	Golgi Matrix Protein
Rat Anti-N-cadherin	RαN-cad	1:10	Cell Adhesion

Guinea Pig Anti-hsc3XN	GpαhscXN	1:100	ER Compartment Marker
Mouse Anti-Prospero	MαPros	1:10	Transcription Factor Involved in Apical/Basal Polarity
Lysotracker (red)	-	1:500	Lysosomes
Mouse Anti-Cut	MαCut	1:100	Cell Fate Regulator
Rabbit Anti-Cleaved Caspase 3	RbαCaspase	1:100	Indicator of Apoptosis
Rat Anti-Senseless	RαSens	1:1000	Pro-Neuronal Protein
Mouse Anti-Chaoptin	Mα24B10	1:20	Surface Glycoprotein on Axons
Mouse Anti-Wrinkled	MαW	1:100	Head Involution Defect/Programmed Cell Death
Rat Anti-K-Del	RαK-Del	1:100	ER Compartment Marker

Secondary Antibody	**Abbreviation**	**Dilution**	**Color**
Anti-Green Fluorescence Protein A^{488}	αGFP A^{488}	1:1000	Green
Anti-Rabbit A^{488}	αRb A^{488}	1:500	Green
Anti-Mouse A^{568}	αM A^{568}	1:500	Red
Anti-Rat A^{647}	αR A^{647}	1:500	Blue
Anti-Mouse A^{594}	αM A^{594}	1:500	Red
Anti-Chicken A^{488}	αChk A^{488}	1:500	Green
Anti-Rat A^{594}	αR A^{594}	1:500	Red
Anti-Mouse A^{488}	αM A^{488}	1:500	Green
Anti-Rabbit A^{647}	αRb A^{647}	1:500	Blue
Anti-Rat Rhodamine	αR Rhodamine	1:500	Red
Anti-Guinea Pig A^{647}	αGp A^{647}	1:500	Blue
Anti-Mouse A^{647}	αM A^{647}	1:500	Blue
Anti-Guinea Pig A^{549}	αGp A^{549}	1:500	Red
Anti-Phalloidin A^{647}	αPhalloidin A^{647}	1:100	Blue (Actin Cytoskeleton)
Anti-Chicken A^{568}	αChk A^{568}	1:500	Red
Anti-Rat A^{488}	αR A^{488}	1:500	Green

Appendix B

SOLUTIONS

- **5X PEM:** 0.1 M Pipes, 2 mM EGTA, 1mM $MgSO_4$ pH adjusted to 6.95 with concentrated HCl and stored at 4°C

- **PEM-FA:** 5X PEM (final 1X), 16% formaldehyde (4% final), distilled water

- **1X Phosphate Buffered Saline (PBS):** 10 mM phosphate (pH 7.4), 183 mM NaCl, 27 mM KCl

- **Hoyer's Mounting Media:** 30 g gum Arabic dissolved in 50 mL H_2O under a fume hood and heated to 60°C. Two-hundred g chloral hydrate is slowly added and dissolved followed by 20 g glycerol. The mixture is centrifuged at 10,000xg, and the supernatant is filtered through glass wool (Selva & Stronach, 2007).

Appendix C

DROSOPHILA CROSSES

Diagram depicting the series of crosses used to generate germline clone embryos used in cuticle preparations and immunofluorescent stainings.

***ALG10*:**

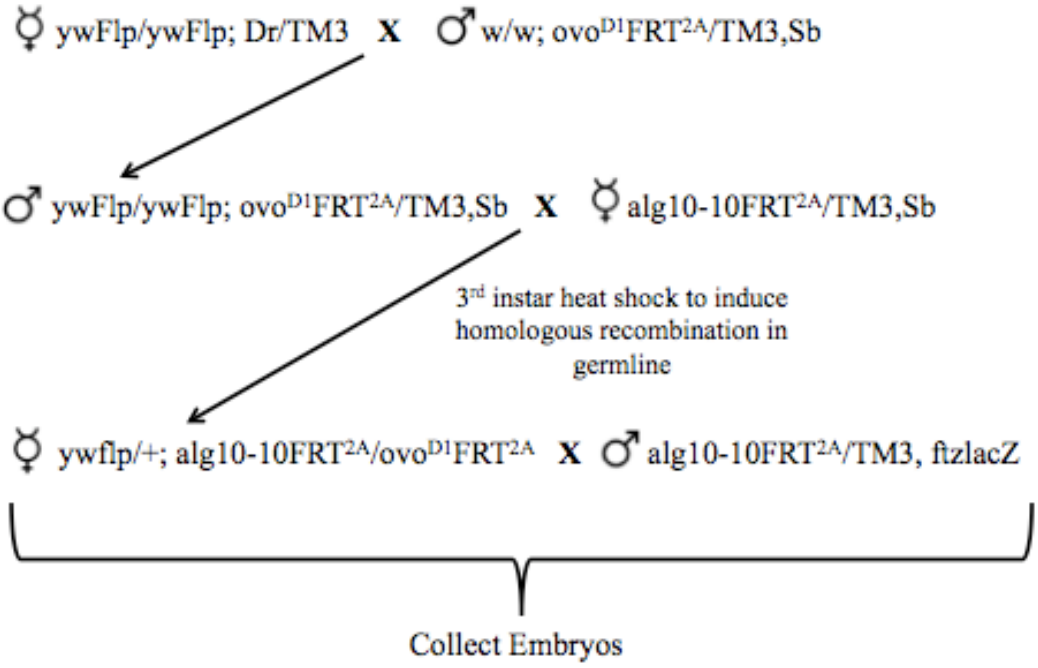

***ALG9*:**

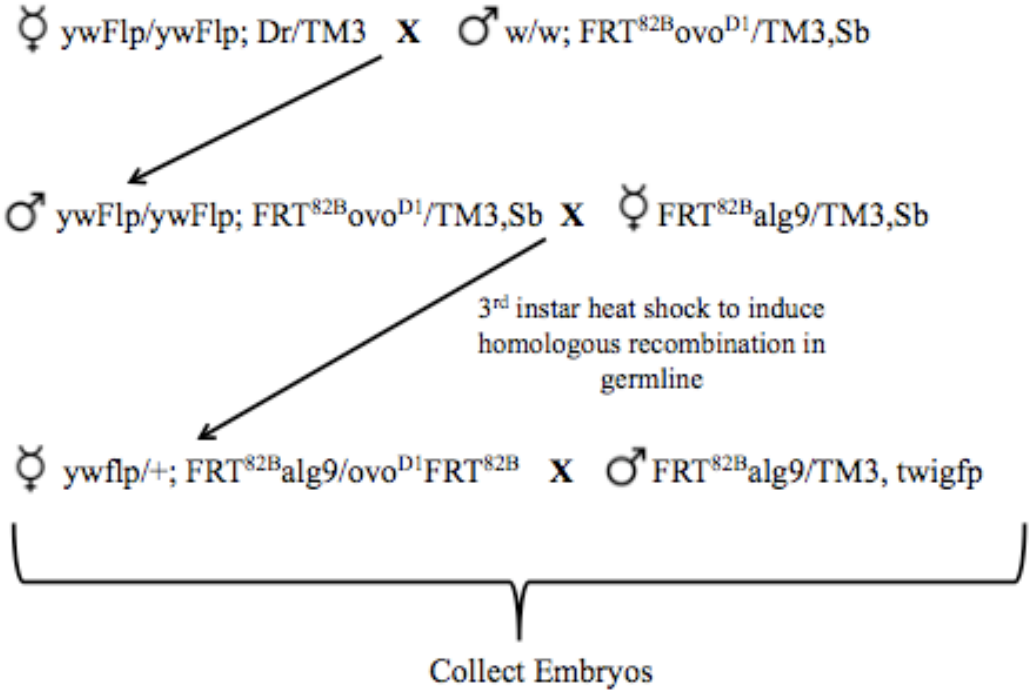
♀ ywFlp/ywFlp; Dr/TM3 X ♂ w/w; FRT82B ovoD1/TM3,Sb
♂ ywFlp/ywFlp; FRT82B ovoD1/TM3,Sb X ♀ FRT82B alg9/TM3,Sb
3rd instar heat shock to induce homologous recombination in germline
♀ ywflp/+; FRT82B alg9/ovoD1 FRT82B X ♂ FRT82B alg9/TM3, twigfp
Collect Embryos

The figure below depicts the crosses used to generate mosaic larvae used for immunofluorescent stainings and adults used for imaging of the rough eye phenotype via the eyFlp method.

***ALG10*:**

♀ eyFlp/eyFlp; eygal4/Cyo; gmrhidFRT^{2A}/TM6C, Sb, Tb **X** ♂ Sp/Cyo; alg10-10FRT^{2A}/TM6C

Homologous recombination occurs in eye tissue only;
Collect Non-Tb 3rd instar larvae and isolate eye discs for antibody staining or Collect Non-Sb rough eye adults for imaging

♀ eyFlp/Cyo; gmrhidFRT^{2A}/TM6B **X** ♂ Sp/Cyo; alg10-10FRT^{2A}/TM6C

Homologous recombination occurs in eye tissue only;
Collect Non-Tb 3rd instar larvae and isolate eye discs for antibody staining or Collect Non-Sb rough eye adults for imaging

***ALG9*:**

♀ yw/yw; eyFlp/(Cyo); FRT^{82B}gmrhid/TM6B **X** ♂ w/w; Sp/Cyo; FRT^{82B}alg9/TM6C

Homologous recombination occurs in eye tissue only;
Collect Non-Tb 3rd instar larvae and isolate eye discs for antibody staining

♀ yw/yw; eyFlp/(Cyo); FRT^{82B}gmrhid/TM6C **X** ♂ w/w; Sp/Cyo; FRT^{82B}alg9/TM6C

Homologous recombination occurs in eye tissue only;
Collect Non-Sb, rough-eye adults for imaging

The following cross was used to demonstrate rescue of the rough eye phenotype in adult *alg10* eyes:

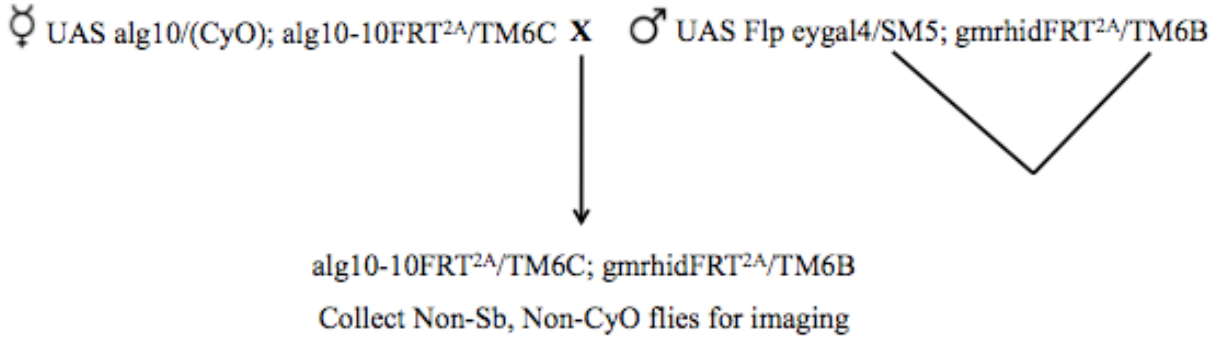

The following complementation cross was performed in order to confirm the presence of the *alg10* mutation. The absence of non-Sb flies out of this cross confirms the presence of alg10-10 at 68A9.